



저작자표시-비영리-변경금지 2.0 대한민국

이용자는 아래의 조건을 따르는 경우에 한하여 자유롭게

- 이 저작물을 복제, 배포, 전송, 전시, 공연 및 방송할 수 있습니다.

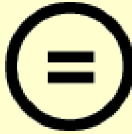
다음과 같은 조건을 따라야 합니다:



저작자표시. 귀하는 원저작자를 표시하여야 합니다.



비영리. 귀하는 이 저작물을 영리 목적으로 이용할 수 없습니다.



변경금지. 귀하는 이 저작물을 개작, 변형 또는 가공할 수 없습니다.

- 귀하는, 이 저작물의 재이용이나 배포의 경우, 이 저작물에 적용된 이용허락조건을 명확하게 나타내어야 합니다.
- 저작권자로부터 별도의 허가를 받으면 이러한 조건들은 적용되지 않습니다.

저작권법에 따른 이용자의 권리는 위의 내용에 의하여 영향을 받지 않습니다.

이것은 [이용허락규약\(Legal Code\)](#)을 이해하기 쉽게 요약한 것입니다.

[Disclaimer](#)

Ph.D. DISSERTATION

Electrical Detection of the Microcystin-LR using Carbon Nanotube Channel

(카본 나노 튜브 채널을 이용한 마이크로 시스템에
대한 전기적 검출)

By

Hyuk Je Kwon

February 2013

SCHOOL OF ELECTRICAL ENGINEERING AND COMPUTER SCIENCE
COLLEGE OF ENGINEERING
SEOUL NATIONAL UNIVERSITY

Electrical Detection of the Microcystin-LR using Carbon Nanotube Channel

(카본 나노 튜브 채널을 이용한 마이크로 시스틴에 대한 전기적 검출)

指導教授 朴 榮 俊

이 論文을 工學博士 學位論文으로 提出함

2013 年 2 月

서울大學校 大學院

電氣-컴퓨터 工學部

權 赫 濟

權 赫 濟의 工學博士 學位論文을 認准함

2013 年 2 月

委 員 長 _____ (印)
副委員長 _____ (印)
委 員 _____ (印)
委 員 _____ (印)
委 員 _____ (印)

Electrical Detection of the Microcystin-LR using Carbon Nanotube Channel

by

Hyuk Je Kwon

Submitted to the School of Electrical Engineering and
Computer Science

in partial fulfillment of the requirements for the degree of
Doctor of Philosophy in Electrical Engineering

at

SEOUL NATIONAL UNIVERSITY

February 2013

© Seoul National University 2013

Committee in Charge:

Sunghoon Kwon, Chairman

Young June Park, Vice-Chairman

Yoon-Sik Lee

Seunghun Hong

Yoondong Park

Abstract

Various types of novel nanostructures have been suggested and explored for real-time and label-free detection processes for biological and chemical sensor applications. Among them, carbon nanotubes (CNTs) are a novel class of nanomaterials that reportedly show good levels of electrical sensitivity to the environmental conditions surrounding a transducer. This property is appropriate for channels of field effect transistor (-FET) devices. Thus, the CNT-FET has been highlighted for use in electrochemical sensors in aqueous solutions.

In this dissertation, we propose a sensor platform that can achieve reliability of a CNN channel and a CNN channel together with gold particles, enhance sensitivity and block protein adsorption on the metal-nanotube contact region in an electrical biosensor.

There are three phases in the study. In the first phase, we investigate the reliable operation of a CNN-based sensor in electrolyte by using a carboxylated CNN-based sensor. The SiOH (silanol) groups on the SiO₂ surface and COOH (carboxyl) groups are known to be protonated and negatively charged in a phosphate buffer solution (PBS) or distilled water. We verify the combined effect of SiOH and COOH groups on CNT conductance by studying acid-base properties of a CNN channel using a unit step voltage technique. In addition, we find the role of the silanol and carboxyl groups and propose a method to enhance the stability of a CNN channel for bio-sensing applications.

In the second phase, we revisit the effect of carbon nanotube density on the

performance of CNN-based FET (CNN chip) by controlling the channel resistance to enhance sensitivity. The enhanced sensitivity is obtained as the channel resistance increases. This shows that the characteristics of low density CNN experiences more electrostatic interaction for the target molecule charge. In addition, we introduce Au nano-particles (AuNPs) as binding sites on the CNN-based FET (CGI chip) and then compare the device performance with CNN-only FET. Clearly, AuNPs-FET shows better performance with a good repeatability.

In the third phase, we propose a 6-mercapto-hexanol (MCH) treatment on an Au electrode surface to block the protein adsorption on the metal-nanotube contact region. Non-specific binding (NSB) is known to occur on both CNN channel and metal-nanotube contact. However, the metal-nanotube contact region is significantly susceptible to the conductance modulation by NSB. For the prevention of protein adsorption on a metal contact, a MCH treatment is introduced to the CNN channel before the Au nano-particles deposition. The MCH-treated device shows approximately 30~ 50% increase in conductance at a 0.5uM target molecule. The result is a surprising contrast to our previous observations in CNN and CGI chips. The enhanced sensitivity can be explained by the elimination of a schottky barrier on the metal-nanotube contact, leading to a significant decrease in the device conductance.

Keywords: CNT-based sensor, CNN channels, AuNPs, MCH, and Sensitivity.

Student Number: 2008-30209

Contents

Abstract	i
Contents	iii
List of Tables	vi
List of Figures	vii
Chapter 1	1
Introduction	1
1.1 Motivation	1
1.2 Au nano-particles (AuNPs)	5
1.3 MCH treatment	6
1.4 Outline of the Dissertation.....	7
Chapter 2	9
Acid-base properties of carboxylated carbon nanotube network	9
2.1 Introduction.....	9
2.2 Electrical characteristics of CNN in PBS	11
2.2.1 The conductance modulation of CNN in PBS.....	12
2.2.2 The fast component	15
2.2.3 The slow component.....	17
2.3 Surface modification	18
2.3.1 A passivation of the oxide surface using APTES.....	18
2.3.2 A capping treatment of the defects using EDC/NHS mixture.....	20
2.4 Conclusion	25
Chapter 3	26
Carbon nanotube network chip: CNN chip	26

3.1 Introduction.....	26
3.1.1 Concentric electrodes and self-gating effect	27
3.2 Sensing of microcystin-LR with CNN chip	30
3.2.1 I-V characteristics of CNN chip.....	30
3.2.2 The effect of EDC and NHS	33
3.2.3 The control experiment with the thrombin molecule.....	36
3.3 Relationship between the resistance and the sensitivity.....	37
3.4 Conclusion.....	39
Chapter 4	40
Carbon nanotube gold island chip: CGI chip.....	40
4.1 Introduction.....	40
4.2 Effect of AuNPs deposition on the CNN	42
4.3 Sensing of microcystin-LR with AuNPs-CNN.....	44
4.3.1 I-V characteristics of AuNPs-CNNFET	44
4.3.2 Effect of thiol-terminated linker (DTSP).....	46
4.4 Relationship between the resistance and the sensitivity.....	47
4.5 Conclusion.....	48
Chapter 5	49
MCH passivation of CGI chip: MCH-CGI chip.....	49
5.1 Introduction.....	49
5.2 The formation of MCH SAM on Au-nanotube contact region.....	51
5.3 Sensing of microcystin-LR with MCH treated AuNPs-CNNFET.....	53
5.4 Conclusion.....	57
Chapter 6	58
Conclusion	58
6.1 Summary.....	58

6.2 Pulsed measurement of the transient state.....	59
6.3 Future Works	63
References	64

List of Tables

Table 1-1. CNT biosensor for proteins.....	4
--	---

List of Figures

Fig. 2-1 (a) A schematic of CNT-based biosensor (b) A schematic vertical sectional view of CNT-based biosensor (c)The SiOH group on the SiO ₂ surface and COOH group on the CNT surface are deprotonated in PBS.	10
Fig. 2-2. (a) current and (b) normalized current the CNT-FET in PBS after application of unit pulse of 0.1V to the drain electrode with the source grounded.....	12
Fig. 2-3. (a) Real-time measurement of current change of CNT-FET in PBS and (b) logarithmic plot after application of the unit pulse of (+) 0.1V unit pulse to the drain with the source grounded.	14
Fig. 2-4. Real-time measurement of current change of CNT-FET: (a) (+) 0.5V unit voltage is applied to the drain, (b) (-) 0.5V unit voltage is applied to the drain. (c) Conceptual diagram (d)-(e) Equivalent circuit models and the diagrams of energy-level alignment	16
Fig. 2-5 (a) Time dependence of the normalized current for pristine CNT and the SiO ₂ surface after being passivated with APTES as shown in (b)	19
Fig. 2-6. (a) The real-time measurement for a pristine CNT-FET in various pH solutions and (b) after the capping of the COOH group on the CNT surface	22
Fig. 2-7. Real-time measurement of the normalized current after application of unit voltage of 0.1V to the drain for various treatment of the CNN channel.....	24
Fig. 3-1. (a) I _{ds} versus V _g curves at V _{ds} = 0.1V in log scale for devices with each channel resistance. (b) Current-versus-V _d curve of the device in the air and in the buffer solution with pH 7.4. The drain is swept from -0.5V to 0.5V with the source grounded. (c) Plot of the self-gating index versus the channel resistance for each device with different channel resistance.....	28
Fig. 3-2. The structure of microcystin-LR.....	31
Fig. 3-3. Schematic structure of an immobilization of antibody on COOH group.....	32
Fig. 3-4. Different scale of conductance drops after the surface modifications of the CNN	

channel. (a) The I-V measurements are processed by a pristine CNN (solid line, black) → after NHS/EDC mixture treatment (dash line, blue) (b) The I-V measurements are processed by an antibody immobilization (solid line, red) → after antigen-antibody reaction (solid line, black).....	32
Fig. 3-5. (a) Real-time measurement result of the carboxylated CNN in PBS with only EDC by applied +0.1V unit voltage and (b) Measurement on the same device with only NHS	35
Fig. 3-6. Ids versus Vds curves before (black) and after (red) exposure to thrombin at the concentration of 0.1uM.....	36
Fig. 3-7. Plots of the sensitivity for each CNN devices with different channel resistance. The sensitivity depends on the channel resistance of CNN-based sensor.....	38
Fig. 4-1. Schematic of an immobilization of antibody on AuNPs-CNN channel.....	42
Fig. 4-2. Conceptual scheme illustration of band diagram for the AuNPs deposition on CNN channel.....	43
Fig. 4-3. Change in device characteristic I_{DS} (V_D) on modification of the AuNPs-CNN surface. (a)I-V curves of the AuNPs-CNN device for different steps; bare CNN (dash line, black), AuNPs-CNN in air (dash dot line, green), AuNPs-CNN in water (solid line, blue), and thiol-terminated linker (dot line, red). (b) I-V curves of the AuNPs-CNN device for different steps; thiol-terminated linker (dot line, red), after antibody immobilization (dash line, black), and after antigen-antibody reaction (solid line, blue). (c) ~ (e) Schematics and corresponding energy band diagrams of the device (c) CNN device: hole carriers are accumulated by the Au electrode (The work function of Au = 5.1eV, work function of swCNT = ~4.8eV) (d) AuNP-CNN device: hole carriers are accumulated in the vicinity of AuNP on the CNN (e) After immobilization of DSP (thiol-terminated molecule), the work function of Au is decreased by DTSP. The schottky barrier increased and the hole carriers are depleted.....	45
Fig. 4-4. The energy-level alignment at Au-S.....	46
Fig. 4-5. Plots of the sensitivity for two types of devices with different channel resistance. Black are for CNN devices and red are for AuNP-devices.....	47
Fig. 5-1. Conceptual scheme of a MCH treated AuNPs CNNFET	51
Fig. 5-2. Conceptual scheme of fabrication flow of three different surface modifications....	52

Fig. 5-3. (a) Change in device characteristic I_{DS} (V_D) on pre-treatment of the MCH-AuNPs-CNN; pristine CNN (solid line, black), MCH-CNN (dash dot line, brown), MCH-AuNPs-CNN (dash line, yellow green), and thiol-terminated liner (dot line, green). (b) I-V curves on sensing measurement of the MCH-AuNPs-CNN device; after antibody immobilization (dash dot line, green), after stop solution (solid line, blue), and after antigen-antibody reaction (dash line, red).....	55
Fig. 5-4. Energy-level alignments during the surface modifications.....	56
Fig. 6-1. Schematics of the potential distribution in an electrolyte (a) low ionic strength (b) high ionic strength.....	60
Fig. 6-2. Comparison of transient response between antibody and antigen after the unit voltage applied.	61
Fig. 6-3 Sensitivity enhancement by transient measurement after 0.5V unit voltage applied.	62

Chapter 1

Introduction

1.1 Motivation

Carbon nanotube (CNT) can be easily fabricated as field-effect transistors (FET) and shows great modulation of electrical properties on exposure to analytes.^{1,2} Therefore, their unique electrical, chemical properties are widely studied so as to develop high performance devices. Single-wall CNT(SWNT)s are divided into metallic and semiconducting tubes according to the chirality of the tube.^{3,4} Semiconducting SWNT is a p-type semiconductor with holes as the main charge carriers and plays an important role in the operation of CNT-based field-effect transistor (CNT-FET).^{5,6,7,8,9} The electrical conductance of a semiconducting CNT is sensitive to its environment and varies significantly with surface adsorption of various chemicals and bio-molecules^{10,11,12,13}. This makes CNT-FET a promising

candidate for label-free biosensing. CNT-FET devices are composed of individual SWNT or CNT network (CNN) between a source electrode and a drain electrode. The conductance of CNT can be modulated by applying a potential of the back gate or liquid gate. CNT-FET based biosensors have been reported to detect various biological proteins.^{14,15,16}

A common method for the detection of proteins is to bind them selectively using antibody–antigen interaction. Two main strategies for antibody immobilization are covalent or non-covalent functionalization. As the covalent method, the CNT are oxidized to make a COOH group for binding with amine group of protein surface by using EDC/NHS.¹⁷ For the non-covalent strategy, a linker molecule is first coated on the CNT surface, and proteins are covalently bound to the linkers. 1-pyrenebutanoic acid succinimidyl ester is first adsorbed onto a CNT via π -stacking interaction, and then proteins are immobilized through a substitution of N-hydroxysuccinimide.¹⁸

The biological recognition-such as antibody-antigen interactions can be measured by electrical measurement of a FET device. The current change at a fixed gate voltage will show the specific binding of target molecules with the antibody immobilized on the CNN channel. The current change is dependent on the charge of target molecules. The charge of bio-molecule is determined by the difference in pH (Δ pH) between pI of bio-molecule and pH of solution. This sensing mechanism is consistent with the gate effect. Table 1 shows the various pI of bio-molecule and different protein biosensors.

The big challenge for CNT-FET based sensor is to implement them for clinical testing and to demonstrate the reliability and reproducibility of the sensor. Two generalized strategies for better designing of CNT-FET sensor are inducing the binding event to occur near the CNN channel and reducing non-specific adsorption. The size of receptor (normal antibody 10~12nm) is usually much larger than the Debye length and target molecule cannot approach the CNT surface. The method to overcome this problem is using small receptors such as aptamer or antibody fragment. In addition, extending the Debye length can be another solution. Non-specific binding (NSB) in FET sensor is a critical issue that will be worse in serum or blood samples. The NSB of proteins to the surface of CNN channel results in a significant conductance decrease and can be explained in terms of the effects of electron doping on the CNT channel^{19,20} and schottky barrier modulation at the metal-nanotube contact¹. This mechanism is inconsistent with the gate effect due to specific binding, and the current change is also contrary to each other. Much more works to be done to overcome the NSB phenomena and a lack of reliable operation in electrolyte solutions.

In this dissertation, we propose a new sensor platform which can support a reliable operation, overcome the NSB phenomena and the enhanced sensitivity. This platform consists of Au nano-particles (NPs) as binding sites and 6-mercapto-hexanol (MCH) treatment for the passivation of Au electrodes. In the following section 1.2 and 1.3, we briefly introduce AuNPs and MCH treatment with our platform.

Table 1-1. CNT biosensor for proteins

Sensor platform	Sensor details	Analyte	pI	LOD	Ref.
ELISA	Fluorescence-linked immunoassay	Streptavidin	5.6~6.8	60pM (3.8ng/ml)	⁹
ELISA (SPR)	Surface Plasmon fluorescence immunoassay	PSA	6.9	80fM	¹¹
Solid-phase microextraction	Time-of-Flight Mass Spectrometry	Microcystin -LR	2	0.8nM (0.8pg/ml)	¹⁶
Electrical sensing (CNT)	SWNT coated with APTES	Streptavidin	5.6~6.8	50nM	^{17, 18}
Electrical sensing (CNT)	Antibody fragment on CNT-FET	IgG	8.6	7.0fM	¹⁰
Electrical sensing (CNT)	Aptamer on CNT-FET	IgE	5.2~5.8	250pM	^{19, 20}
Electrical sensing (CNT)	CNT-FET with spacer between antibodies	PSA	6.9	30pM (1.0ng/ml)	^{21, 22}

1.2 Au nano-particles (AuNPs)

Among the novel metal nano-particles, gold has received great attention owing to its catalytic properties and chemical stability in electrochemical sensors and biosensors.^{21,22,23,24} The increase of the surface area and the catalytic activity were achieved by combining Au nano-particles (AuNPs) with CNTs. AuNPs were introduced as electro-catalyst and CNTs were used as a working electrode.

However, we propose Au nano-particles (AuNPs) as binding sites and CNT network (CNN) as channel of FET device. The number of AuNPs is precisely controllable and AuNPs are distributed uniformly on CNN channel by the thermal evaporation process. Antibodies can be immobilized on the AuNPs by using the thiol-terminated molecule (DTSP) as a linker. The AuNPs-device is incubated with DTSP solution (4 mg/ml⁻¹ in dimethyl sulfoxide) during 30min.²⁵ DTSP contains a thiol group which forms the stable S-Au and a highly reactive succinimide ester. The AuNPs decorated devices (CGI chip) clearly offer high sensitivity even for CNN resistance higher than 30k Ω . The density of Au nano- is about 7.0×10^{11} ea/cm² with the size of 5~7nm. As the size of the antibody is 12nm, only one antibody can be immobilized on one Au nano-particle, in which we can precisely control the number of antibodies on the channel region. This data suggest that we can improve the sensitivity and reproducibility of the sensor by introducing Au particles on the CNT network as the binding site.

1.3 MCH treatment

Previous studies on protein adsorption have shown that many different types of proteins adsorb spontaneously onto carbon nanotubes from aqueous solution.^{1,26,27} The significant conductance change of single-wall carbon nanotubes in response to the physisorption of ammonia and nitrogen dioxide demonstrates their ability to act as extremely sensitive. This adsorption results in a decrease in the electrical conductance of the nanotube. The modulation of conductance due to Non-specific bonding (NSB) is known to occur on both carbon nanotubes and the metal-tube contact.¹ Much of the conductance changes due to protein adsorption originate from the metal-tube contact region.

However, the device which the metal-tube contact regions are protected from NSB by polymer behaves differently. This discrepancy is explained by the elimination of Schottky barrier of the metal-nanotube contacts due to NSB.

In this study, we propose a passivation of Au electrode by self-assembled monolayer (SAM). We introduce a 6-mercapto-hexanol (MCH) as SAM for the passivation of Au electrode-tube contact region. By the elimination of NSB, the enhanced sensitivity was obtained with microcystin-LR sensing in distilled water.

1.4 Outline of the Dissertation

This dissertation is organized as follows.

In chapter 2, an acid-base property of carboxylated CNN is described. We passivate the silanol sources on the SiO₂ surface by organo-functional silane (APTES) and block the CNT defects to make the CNN-FET device insensitive to the pH condition. As the unwanted side reactions are reduced by the surface treatments of the oxide and CNTs, a reliable operation and sensitivity of the sensor are guaranteed.

In chapter 3, antibody is immobilized to the COOH on the CNT surface. For the sensitivity enhancement, the CNN channel resistance is tuned by the controlling the CNT coating rate. We obtain the result that the sensitivity is proportional to the CNN channel resistance.

In chapter 4, Au nano-particles are introduced to CNN chip. To improve the sensitivity fluctuation due to defect distribution on the CNTs surface area, we use Au nano-particles as binding sites. Through the thiol-terminated linker (DTSP), we investigate the sensing performance of AuNPs decorated devices. It will be shown that introduction of the Au particles on the CNN channel greatly enhances the uniformity among chips fabricated among different lots as well as sensitivity.

In chapter 5, we present the enhanced sensitivity of the electrical microcystin-LR sensing by applying MCH treatment on the Au electrodes surfaces. With the elimination of NSB on Au electrode-tube contact region, we achieve the sensitivity

maximization in our platform.

In chapter 6, conclusions, pulsed measurement of the transient state and suggestions for the further works are given.

Chapter 2

Acid-base properties of carboxylated carbon nanotube network

2.1 Introduction

To investigate the reliable operation of CNN-based sensor in electrolyte, we focus the acid-base properties of CNN channel. In this paper, we used a carboxylated CNN-based sensor and analyzed the conductance property of a CNT-FET using a unit step voltage technique. For the CNN-based sensor, the SiOH (silanol) group on the SiO₂ surface and a COOH (carboxyl) group are known to be protonated and negatively charged in phosphate buffer solution (PBS), as shown in Fig. 2-1. Among them, the silanol groups located at close proximity to the CNT (within the electrical double layer) will cause the accumulation of charge carriers in

the p-type CNT and will thus enhance the CNT conductance. However, the COOH group on the CNT surface will be deprotonated in the PBS, whereas the defect (COO⁻ function) can play as the important role in the pH-sensing mechanism in the CNT-FET. ²⁸ We investigate the combined effect of SiOH and defect on CNT conductance by studying the current response to the unit-step voltage in solutions of various pH levels. Also, the current responses are measured after several surface modifications which selectively passivate each component. From the surface treatments, we verify the role of the silanol and carboxyl groups and propose a method to enhance the stability of a CNT-FET for bio-sensing applications.

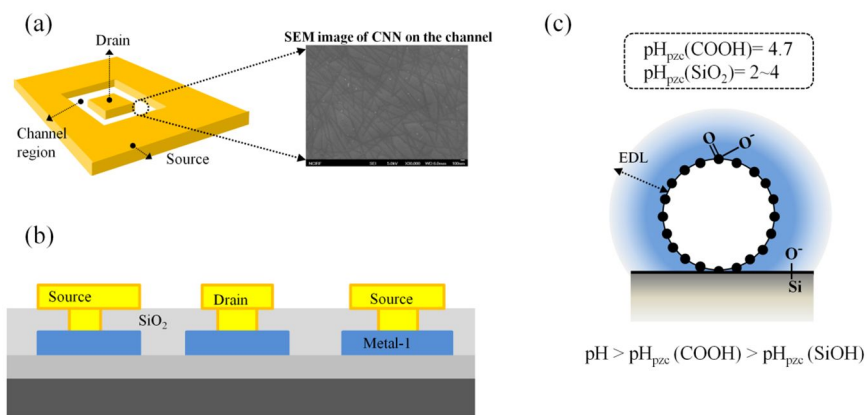


Fig. 2-1 (a) A schematic of CNT-based biosensor (b) A schematic vertical sectional view of CNT-based biosensor (c)The SiOH group on the SiO₂ surface and COOH group on the CNT surface are deprotonated in PBS.

2.2 Electrical characteristics of CNN in PBS

To form a channel between the two electrodes, a CNT network (CNN) is deposited through a dip-coating process.²⁹ An O₂ plasma treatment is applied to promote the uniformity of the nanotube coating. CNT from Hanwha Nanotech Co. was used in this experiment. The CNN is assumed to contain metallic and semiconducting tubes at a ratio of 1:2.³⁰ The CNNs used in our experiment are treated in HNO₃ for 30 min. They were suspended in 1, 2 dichlorobenzene by a sonication. Amino-propyl-triethoxy-silane (APTES), 1-(3-(dimethylamino)-propyl)-3-ethyl carbodiimide hydrochloride (EDC), and N-hydroxy-succinimide (NHS) from Sigma-Aldrich Co. were used. All chemicals were used without further purification. To passivate the carboxyl group on the CNT surface, a 50 μ l droplet of fresh 1mM EDC and 2mM NHS in buffer are placed onto the CNT-FET array and washed off after 30 min.¹⁷ Depending on the measurement method and purpose, the devices are run in real-time mode and/or in the I_d-V_d mode. For electrical measurement of the devices, the CNN-based sensor was stabilized in phosphate buffer solution (PBS) and wired to a semiconductor parameter analyzer (4156C, Agilent).

2.2.1 The conductance modulation of CNN in PBS

We fabricated a CNN-based FET as the transducer device for bio-molecule detection. However, we found that pristine CNN showed a self modulation of conductance in aqueous solution. Fig. 2 shows the time-current measurement of the pristine CNT-FET in the PBS, where the x-axis represents the time passed from the rise of (+) 0.1V unit step- voltage at the drain electrode. It should be noticed that the current decreases continuously with time. The data are not shown here, but the trend is consistent with distilled water.

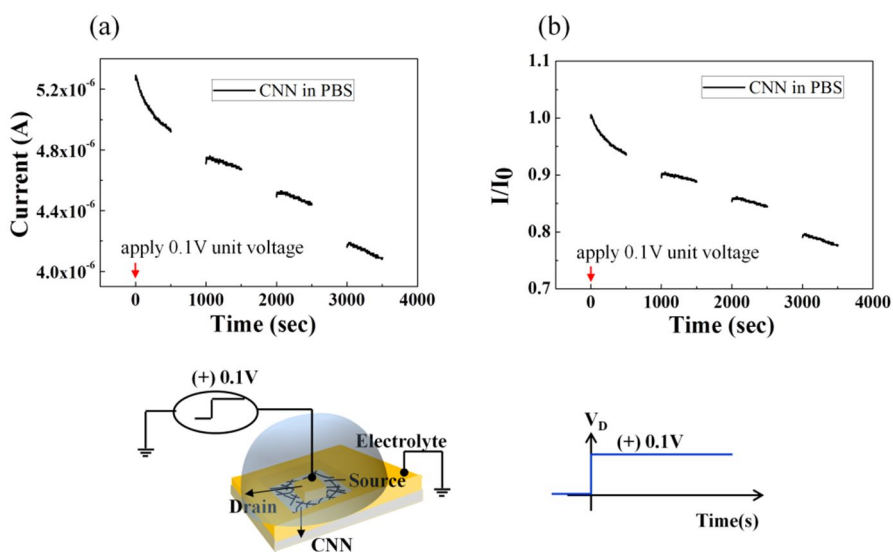


Fig. 2-2. (a) current and (b) normalized current the CNT-FET in PBS after application of unit pulse of 0.1V to the drain electrode with the source grounded.

We treated the CNN with HNO_3 for 30 min for CNN dispersion before using our experiment. Thus, we speculate that the charged surface functional groups near the CNT are due to the decrease in current. The COOH groups (defects) on the CNT surfaces and silanol groups (SiOH) on the SiO_2 substrate are protonated or deprotonated depending on the solution pH. Therefore, the CNN channel current can be a function of surface potential of the charged functional groups.

To verify the current modulation mechanism of CNN in the PBS, a (+) 0.1V unit voltage is applied to monitor the real-time change in the CNT conductance. Fig. 3 shows the real-time measurement of current change of the CNT-FET in the PBS. We observe that the current signal is composed of two components; the fast component shows a sudden increase in the current instantaneously after the pulse and the slow component shows a decrease in the current with long time constant.

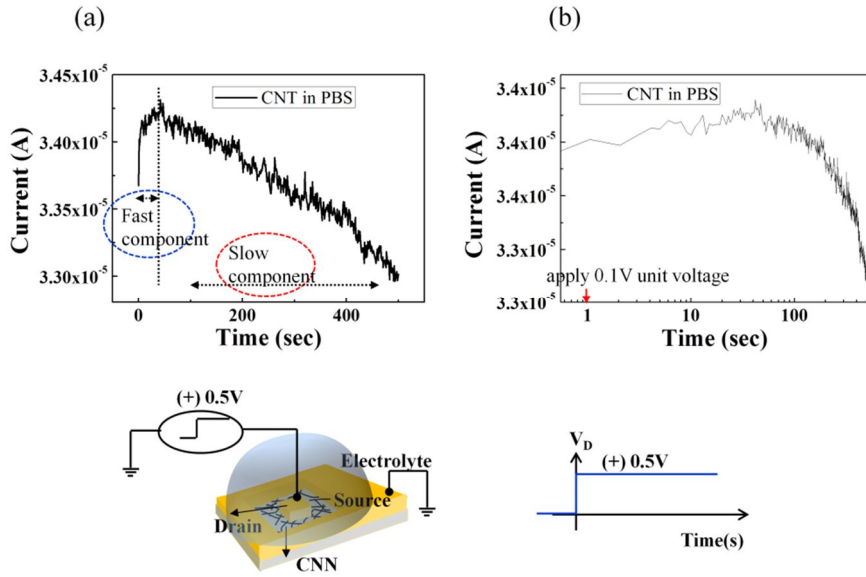


Fig. 2-3. (a) Real-time measurement of current change of CNT-FET in PBS and (b) logarithmic plot after application of the unit pulse of (+) 0.5V unit pulse to the drain with the source grounded.

2.2.2 The fast component

In order to investigate the fast component, we applied (+), (-) 0.5V unit voltage to the drain electrode separately. Fig. 4(a) shows the fast component at (+) 0.5V voltage. It is analogous to the typical response of an ISFET³¹ where the surface charges of SiO₂ layer are monitored by the FET channel conductance change. Therefore, we speculate that the fast component due to the surface functional groups of SiOH on the SiO₂. As we apply a unit voltage, the surface potential at a local point of the CNN also change. If the amplitude of the applied voltage is ΔV , the local potential rises by $k\Delta V$ ($0 < k < 1$) depending on the distance from the drain electrode. The intensity of the induced electric field depends on the distance from the drain electrode by electrostatic potential between the liquid gate and the CNN channel. We focus on the role of mutual electrostatic attraction or repulsion between charged protons and CNN channel according electric field. By adjusting the voltage of the drain electrode, the positive charged protons are repelled from the CNN channel by the induced electric field in fig. 4 (d). The local pH change is induced and SiOH groups will immediately react to this pH change, resulting in the proton release from the SiOH groups. The increase in the current is explained by the field effect due to the increased negatively charged silanol group (SiOH)³² on the oxide surface. Because the point of zero charge of SiO₂ is $\text{pH}_{\text{pzc}} = 3.0$ ^{33,34,35,36}, the acidic silanol groups are likely to be deprotonated in PBS (at pH=7.4), and their negative charges (-SiO⁻) will cause an accumulation of charge carriers in the p-type CNT and will increase the current.

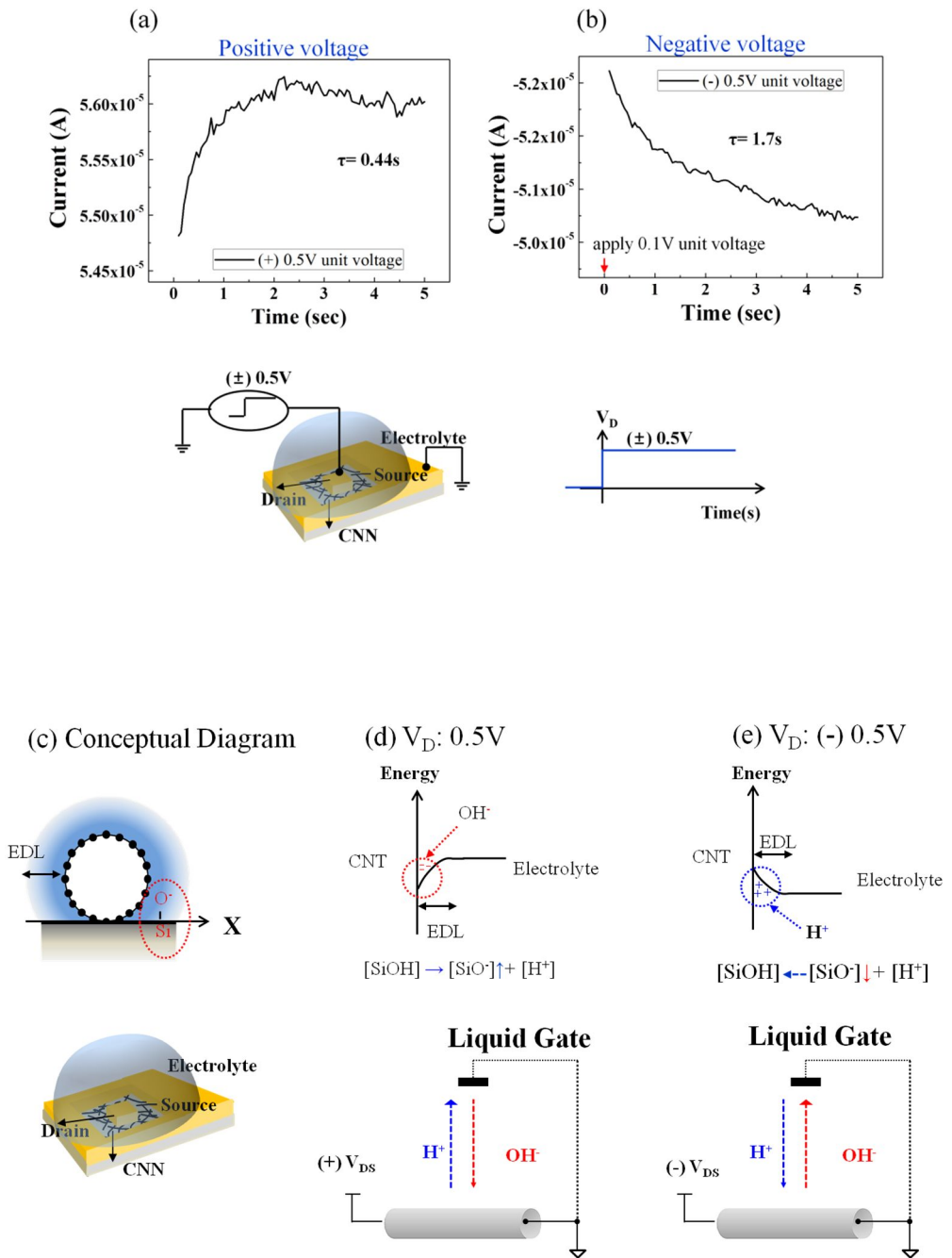


Fig. 2-4. Real-time measurement of current change of CNT-FET: (a) (+) 0.5V

unit voltage is applied to the drain, (b) (-) 0.5V unit voltage is applied to the drain. (c) Conceptual diagram (d)-(e) Equivalent circuit models and the diagrams of energy-level alignment

However, the principal problem is that the charged silanol groups, especially located in the vicinity of the CNT, are not effectively screened by the ions in the solution. After (-) 0.5V unit pulse voltage, the positive charged protons are attracted to the CNN channel and the concentration of proton and the local pH change.³¹ Contrary to the (+) 0.5V pulse, surface hydroxyl groups uptake protons and exhibit a negative transient, so the initial peak shows a decrease in conductance, as shown in fig. 4 (b) and (e).³⁷

2.2.3 The slow component

However, the slow component, as shown in Fig. 2-3(a), shows a decrease in the current with long time constant after the fast current increase. This result can be explained by the negatively charged carboxyl group (COO^-) on the CNT surface. The pH-sensing mechanism for a CNN-based chemical sensor is generally known to be the protonation/deprotonation status of COOH on the CNT surface.⁵ Carboxyl group partially dissociates into H^+ and RCOO^- in PBS (pH 7.4), and the H^+ dissociation (deprotonation) which occurs in the carboxylated CNT can be

considered as the undoping of the hole. The protonation/deprotonation of carboxylic groups on the surface of CNT is considered as hole doping/undoping as charge carriers.³⁶

2.3 Surface modification

To verify that the conductance modulation of the CNN channel is caused by these two functional groups, we carried out two supplementary experiments. First, in order to confirm that the fast component is due to silanol on the oxide surface, a chemical treatment was done on oxide surface with amino-propyl-triethoxy silane (APTES). The second experiment was designed to observe the current change of the CNN channel after the capping of the defect with EDC/NHS mixture.¹⁷

2.3.1 A passivation of the oxide surface using APTES

A self-assembled monolayer (SAM) formation usually is used to modify surface properties in the electrochemical sensors applications, and one of the most commonly used SAM is a organosilane monolayer on hydroxyl surfaces such as oxide surface. A chemical modification of SiO₂ surface by organo-functional silane is a well-known technique for biosensor application.^{38,39} Among them, APTES is

widely used as interfacing molecules. In aqueous solution, the amino-silanes undergo hydrolysis and polymerization in the bulk phase before forming bonding with SiOH of oxide surface.⁴⁰ Therefore, we propose an anhydrous silanization which can offer a homogenous monolayer of the amino-silane on the oxide surface. In, our experiment, the oxide surface of CNN-based sensor may have different charge densities depending on the ionization of silanol groups ($-\text{SiOH}$).

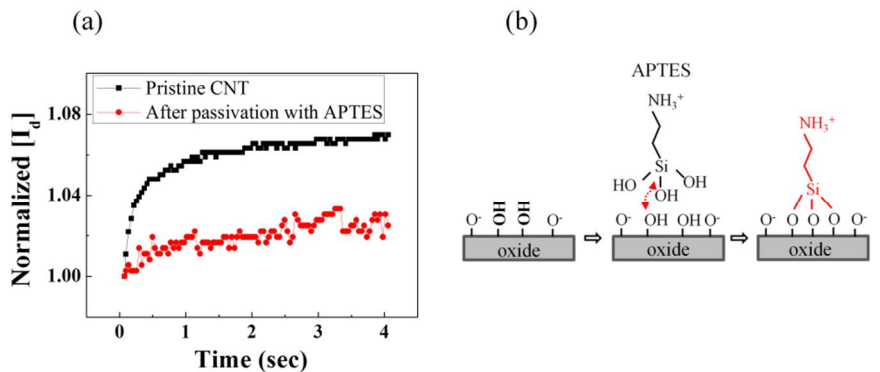


Fig. 2-5 (a) Time dependence of the normalized current for pristine CNT and the SiO₂ surface after being passivated with APTES as shown in (b)

A surface modification with APTES must consume SiOH functional groups on the oxide surface and should change the charge density at the surface. To modify the oxide surface of the channel region, a CNN-based sensor was soaked in an

anhydrous ethanol solution containing 2% APTES for 1hr, followed by a rising process under an alcohol flow.⁴¹ APTES has an amine group that will be protonated and positively charged in an aqueous solution. An APTES treatment can induce a positive charged site on the oxide surface and decrease the negative net charge from the silanol groups on the oxide surface as shown in Fig. 5(a). After the surface modification of the CNN-based sensor with APTES, we observe that a current increase is reduced appreciably, as shown in Fig. 5(b). Therefore, it is clearly confirmed that the fast component of the current signal is due to the effect of the silanol group on the oxide surface.

2.3.2 A capping treatment of the defects using EDC/NHS mixture

The pH-sensing mechanism adopted in a carboxylated CNT-based chemical sensor has been generally known to be due to a defect functional group, especially COOH.⁴² The CNN used in our experiment are treated in HNO₃ for 30min, so it is estimated that the carboxyl group (COOH) is introduced on the CNT surface. In general, COOH group is deprotonated to SiO⁻ and negative charged correspondingly to the difference between the bulk pH and the isoelectric pH (pH_{iep}) of the COOH.

The carboxylated CNT is a p-type semiconductor and the protonation/deprotonation is interpreted as the hole doping/undoping.^{43,44} To investigate the relation between the deprotonation status of COOH groups on the CNT surface and

conductance change of CNN, we measured the current change of CNN channel with several devices for each different pH values. Fig. 6 (a) shows the real-time current measurement of CNN-based sensor with different pH buffer solutions. This suggests that the conductance property of the CNT is expected to be affected by the pH value of solution. The CNT-FET conductance decreases as pH value increases. The current is significantly dependent on pH and protonation/ deprotonation of COOH plays a role of the conductance change of CNN channel. It can be explained by the fact that the COOH group is fully associated at pH 3, and COOH partially dissociates into H^+ and $RCOO^-$ at pH 7, while H^+ is fully dissociated from the COOH group at pH 9.

In order to verify the role of COOH group, we carried out a capping treatment for COOH group on the CNT surface. We passivated the COOH defects of the CNT by the EDC/NHS treatment. 1-(3-(dimethylamino)-propyl) - 3-ethyl carbodiimide hydrochloride (EDC) is a cross-linking agent, used to convert COOH groups to amine-reactive NHS ester in the presence of N-hydroxy-succinimide (NHS).⁷ Therefore, EDC/NHS treatment is usually used to prepare surface modification in biosensor application. After this treatment, a significant current decrease disappears as shown in Fig. 6 (b). This result is sharp contrast to our previous observations in fig. 6 (a). We attributed the pH independent behavior of CNN to a capping of defect. This experiment clearly demonstrates the role of the COOH group on the conductance property of the carboxylated CNN channel in aqueous solution.

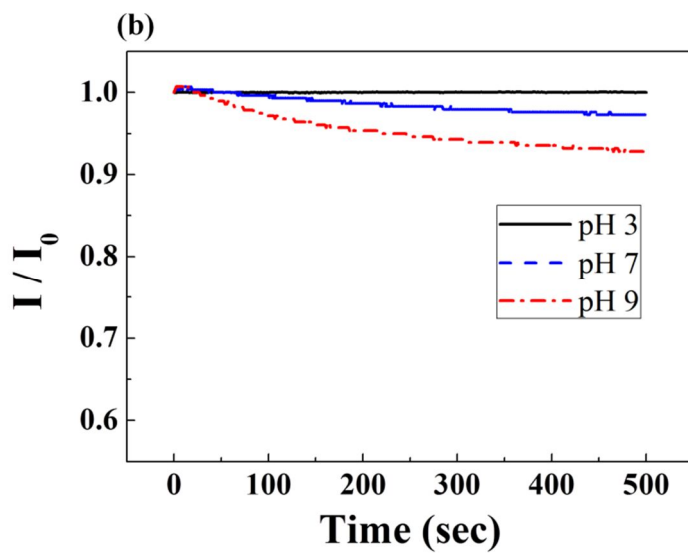
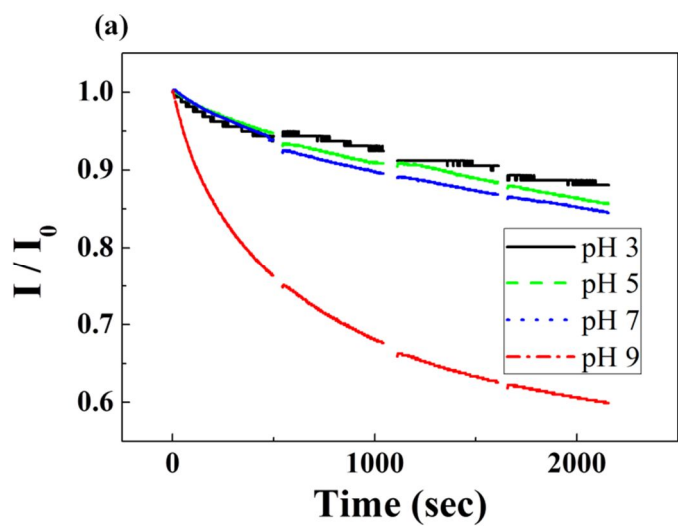


Fig. 2-6. (a) The real-time measurement for a pristine CNT-FET in various pH solutions and (b) after the capping of the COOH group on the CNT surface

This pH-dependent behaviour of the CNN is an undesirable side reaction in a biosensor application. Therefore, we suggest that a capping treatment of COOH defects on CNT surfaces is a promising method to obtain a reliable operation of the biosensor adopting CNN channel. Furthermore, we propose that the defect of CNT may be useful for binding sites of antibody immobilization. COOH may be reacted to NHS in the presence of an EDC, resulting in an intermediate species which can react with amine group of protein surface. After covalently attachment of IgG antibodies to COOH groups (defects), the change in channel current was measured by the time-current measurement before and after antibody immobilization, as shown in fig. 7. After antibody immobilization on the COOH, we would like to emphasize that the CNN channel became fully insensitive with pH condition.

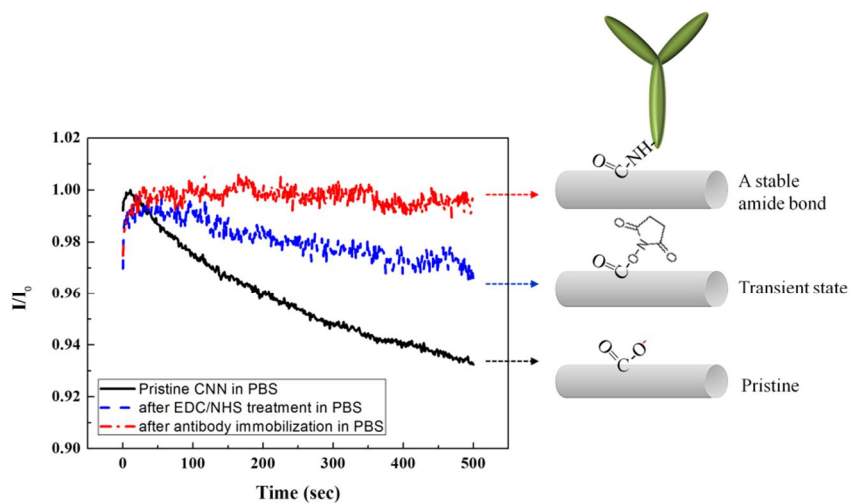


Fig. 2-7. Real-time measurement of the normalized current after application of unit voltage of 0.1V to the drain for various treatment of the CNN channel.

2.4 Conclusion

In this study, we have shown a conductance property of the carboxylated CNN being modulated depending on pH condition in aqueous solution, and verified two types' noise sources of the CNN-based biosensor. The first noise source is the negative charged silanol (SiOH) group at the oxide surface on which the CNTs are located. The 2nd noise source is the COOH functional groups on the CNN surface.

As the noise sources may be the source of a false signal to a protein sensor, the noise sources should be removed. Thus, we passivated the silanol sources on the SiO₂ surface by organo-functional silane (APTES) and blocked the CNT defects to make the CNT device insensitive to the pH condition. As the unwanted side reactions were reduced by the surface treatments of the oxide and CNTs, reliable operation and sensitivity of the sensor could be guaranteed.

Chapter 3

Carbon nanotube network chip: CNN chip

3.1 Introduction

Single-walled carbon nanotubes (SWNTs) have been a subject of numerous studies that are focused on various nanoscale devices due to its superior performance and good electrical sensitivity to environmental conditions.^{11,12,13,25} For electronic applications of SWNT such as gas, pH, DNA, and protein sensors, the carbon nanotubes field effect transistors (CNT-FET) using random network films are highlighted.^{10,45} Several experimental studies have shown that the density of

nanotubes is an important parameter which is related to the performance of the CNN based sensor.^{5,6,7,8}

To further investigate the role of the nanotube density, we revisit the effect of carbon nanotube (CNT) density on the performance of CNN-based FET by controlling the channel resistance. Consistent with the previous works,^{6,7,8} the sensitivity is enhanced as the channel resistance is increased in a low channel resistance regime.

3.1.1 Concentric electrodes and self-gating effect

We used concentric CNN devices for the experiment because the potential of liquid gate can be controlled without the gate electrode (known as the self gating effect).^{46,28} To understand the basic electrical property of the CNN channel, we measured the channel current to determine whether the CNN exhibits a semiconducting or metallic behavior in the air. In order to see the gate modulation in the air, we fabricated a device with 100Å thickness of gate oxide, and used the silicon substrate as a back-gate. The CNN is assumed to contain metallic and semiconducting tubes at a ratio of 1:2.⁸ We change the CNN density by controlling the dipping speed of the CNT coating and the density can be identified by the channel resistance. The device with high channel resistance exhibits the electrical behavior of low CNN density, and a device with low channel resistance exhibits that of high CNN density. The typical plots of source-drain current (I_{ds}) vs. back gate

voltage (V_g) at V_d of 0.1V are shown in fig. 3-1 (a) each channel resistance. The device with high channel resistance shows a high on/off ratio of 10^{2-3} , while that with the low resistance showed a low on/off ratio (<10). This result is consistent with the previous experimental observations and theoretical simulations with according to the percolation theory of CNN.^{5,7,7} The on/off ratio is known be an important parameter to enhance the sensitivity because a high on/off ratio signifies more semiconducting properties of CNN.

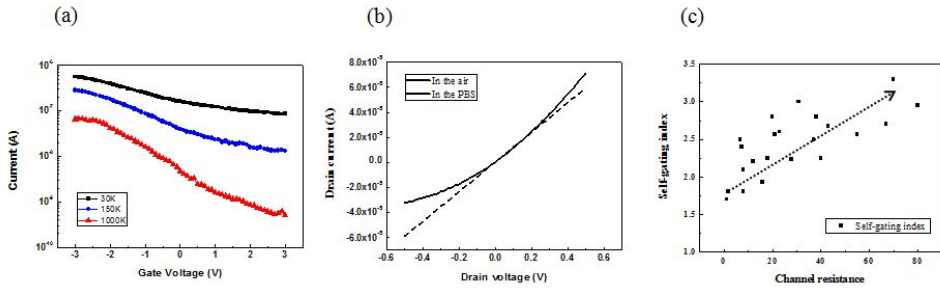


Fig. 3-1. (a) I_{ds} versus V_g curves at $V_{ds} = 0.1V$ in log scale for devices with each channel resistance. (b) Current-versus- V_d curve of the device in the air and in the buffer solution with pH 7.4. The drain is swept from -0.5V to 0.5V with the source grounded. (c) Plot of the self-gating index versus the channel resistance for each device with different channel resistance.

Now, we conduct the experiments in a PBS without the additional gate electrode. As the electric potential of the aqueous solution follows the enclosing electrode

potential, the device shows the self-gating effect^{10, 11} as shown in fig. 3-1(b). Instead of the on/off ratio, a self-gating index is introduced to predict the device performance. It can be explained as follows. While the linear and symmetric I_{ds} vs. V_{ds} curve is observed in the air (dotted line in fig. 3-1(b)), the current is asymmetrically bended as the bias changes in the phosphate buffer solution at pH 7 (solid line in Fig. 3-1(b)). This is due to the fact that the liquid gate potential is highly capacitive coupled with electrode source. Hence, the positive drain (island electrode) voltage and grounded source (surrounding electrode) lead the negative liquid gate potential on the p-type CNN channel, so that hole density and the current of the CNN are increased. On the other hand, for the negative drain voltage, a positive liquid gate potential depletes the hole carrier on the p-type CNN channel and induces less channel current.

By the using this asymmetric conductance property of CNN in a PBS, we define the self-gating index for the concentric device as follows:

$$\text{Self-gating index} = I_{(+0.5V)} / I_{(-0.5V)}$$

From fig. 3-1(c), it can be seen that the self-gating index increases as the channel resistance increases. Therefore, by measuring the self-gating index, we can estimate the semiconductor property of the CNN and investigate the correlation between the sensor performance and channel resistance.

3.2 Sensing of microcystin-LR with CNN chip

3.2.1 I-V characteristics of CNN chip

In order to investigate the sensing performance of CNN-based devices, we used microcystin-LR-BSA conjugates as target molecules. Microcystin-LR is a toxic material, and is considered a bio-indicator when measuring water pollution levels. Thus, the detection of target molecules was carried out in distilled water instead of in PBS. For electrical measurements of the devices, the chip was stabilized in 0.1 M PBS and wired to a semiconductor parameter analyzer (4156C, Agilent). The drain is swept from -0.5V to 0.5V while the source is grounded. The iso-electric point (pI) of microcystin-LR is 2,⁴⁷ so microcystin-LR has a strong negative-charge in a distilled water (pH 6.0) environment, as shown in Fig. 3-2. Antibodies can be covalently bound to COOH groups (defects) on the CNTs surface by EDC/NHS mixture, as shown in Fig. 3-3.¹⁷ A droplet of PBS containing 0.5 μ M microcystin was incubated with the antibody immobilized sensor chip during 15min. After washing with distilled water, the current change was measured by a DC sweep measurements before and after antibody-antigen reaction. Sensitivity can be defined as,

$$\text{Sensitivity} = \Delta I / I_{sd}$$

We measured the current change of the CNN device for each step during surface modifications; bare CNN, after NHS/EDC mixture treatment, after immobilization of antibody, and after antigen-antibody reaction as shown in Fig. 3-4 (a) and (b). Before the measurement of each step, the device was rinsed and incubated with distilled water. After the NHS/EDC mixture treatment, a significant current decrease was observed, which can be explained by the adsorption of EDC on nanotubes.

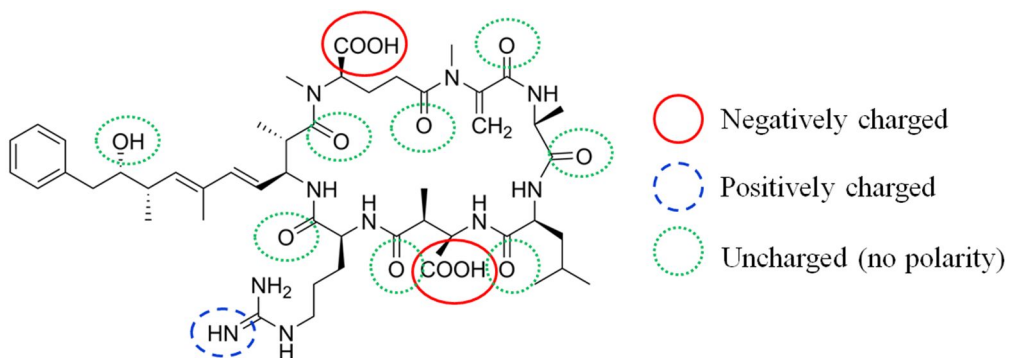


Fig. 3-2. The structure of microcystin-LR

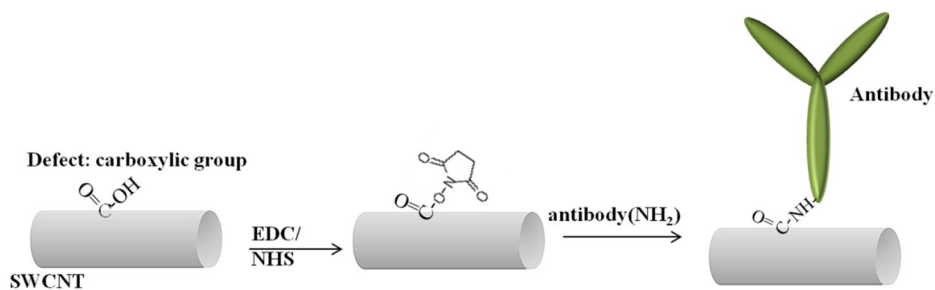


Fig. 3-3. Schematic structure of an immobilization of antibody on COOH group

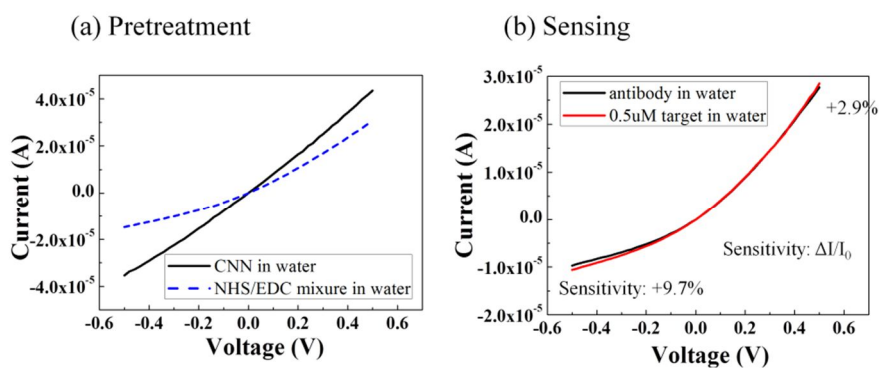


Fig. 3-4. Different scale of conductance drops after the surface modifications of the CNN channel. (a) The I-V measurements are processed by a pristine CNN (solid line, black) \rightarrow after NHS/EDC mixture treatment (dash line, blue) (b) The I-V measurements are processed by an antibody immobilization (solid line, red) \rightarrow after antigen-antibody reaction (solid line, black).

After immobilization of the antibody, current decrease as much as 30% was observed. It is speculated to be due to decrease in the capacitance between the CNN channel and the liquid gate, which decreases the current driving capability. After washing, a 7.8% sensitivity ($\Delta I/I$) was observed for the device with the channel resistance of 12k Ω . The current increase is explained by the field effect where the negative charge of the target molecule induces a hole current on the CNT channel.

3.2.2 The effect of EDC and NHS

The carboxylated CNT is well known to provide the means for particularly sensitive electronic transduction of chemical events.^{36,37} An enhanced scattering at the functionalized site (defect) can play roles in converting chemical changes into conductance changes.⁴⁸

The device showed a 60% decrease in current after exposure to NHS/EDC mixture as shown in Fig. 3-5. We attribute both a defect on the CNT surface and EDC molecule to the source of the decrease in conductance. The defect (COOH) on the CNT surface is known to sensitive scattering site for its chemical environment events, so EDC reacts with a carboxyl group on the CNT surface to form an amine-reactive intermediate species. This intermediate species play roles as enhanced scattering site.

In addition, the amine groups of EDC donate electrons to p-type semiconducting

nanotubes, thereby decreasing conductance, because EDC has free tertiary amine groups.

To examine this speculation, we carefully monitored the current change of carboxylated CNN device in PBS with only 100 μl EDC and only 100 μl NHS separately. Fig. 3-5 shows representative current curves from 30-minute measurement of a carboxylated CNN. Fig. 3-5(a) shows measurement taken with only 100 μl EDC. We confirmed that conductance data shows a rapidly decrease in current. However, the same device exhibited different behavior when only 100 μl NHS was present in Fig. 3-5(b). A significant decrease in conductance during the EDC/NHS treatment step of CNN- FET illuminates that the COOH group form an amine-reactive intermediate species.

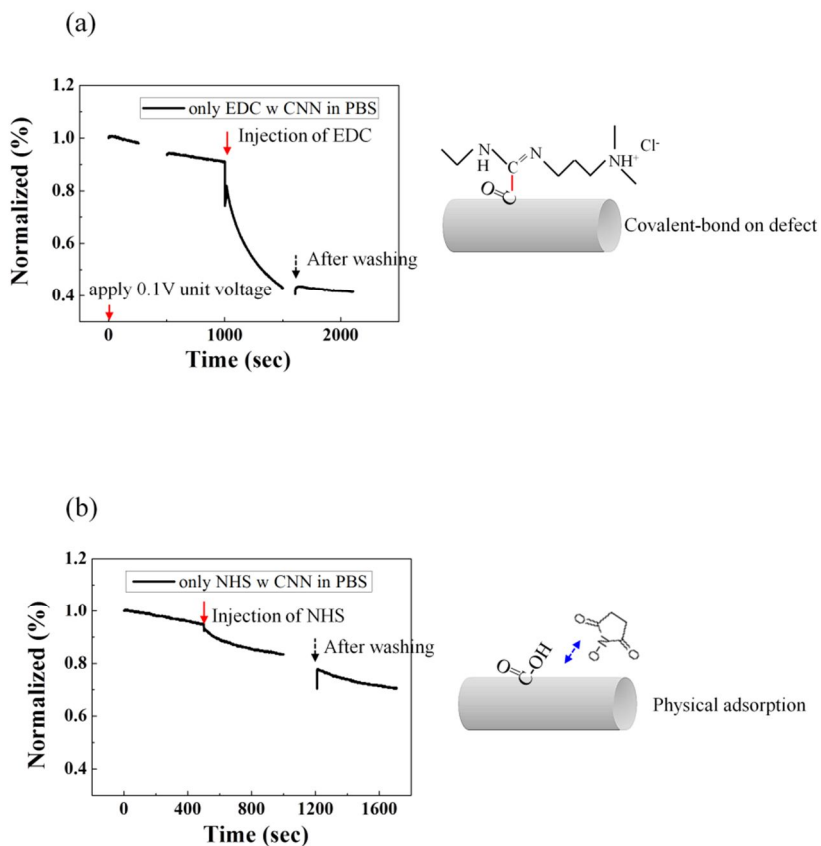
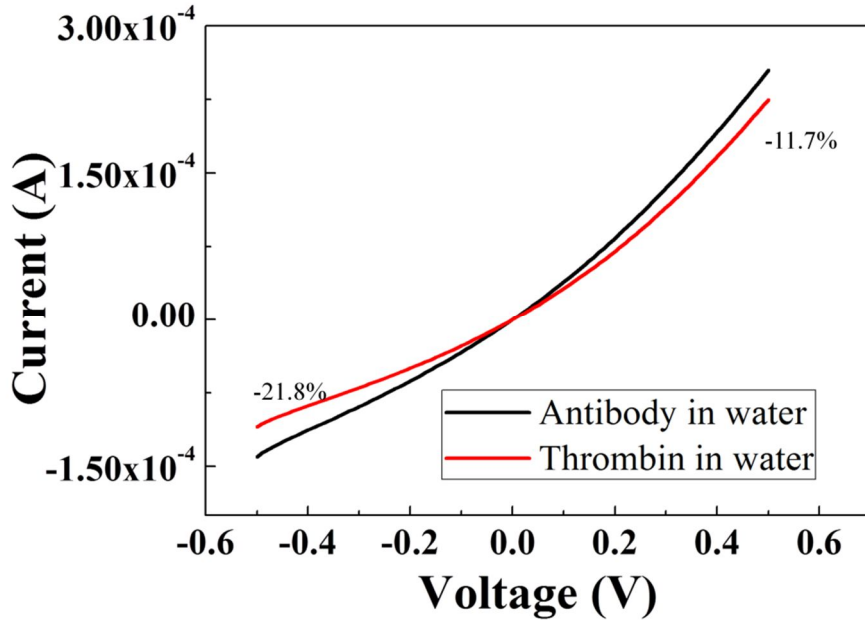


Fig. 3-5. (a) Real-time measurement result of the carboxylated CNN in PBS with only EDC by applied +0.1V unit voltage and (b) Measurement on the same device with only NHS

3.2.3 The control experiment with the thrombin molecule

The control experiment was studied with thrombin molecules using the microcystin antibodies immobilized CNN chip. As the thrombin has no affinity for the microcystin antibody, thus it induced a decrease in current due to the non-specific binding (NSB) on the CNT surface as shown in Fig. 3-6.



. Fig. 3-6. Ids versus Vds curves before (black) and after (red) exposure to thrombin at the concentration of 0.1uM

The device showed a 20% decrease in conductance after exposure to 0.1 μ M thrombin. Non-specific adsorption of proteins on carbon nanotubes occurs spontaneously and irreversibly in an aqueous solution.^{1,27} This NSB shows conductance changes of CNT and induces false signals in CNT-based biosensors. Thus, a blocking layer should be introduced to our CNN-based sensor system to block the device from NSB.

3.3 Relationship between the resistance and the sensitivity

To verify the correlation between sensitivity and a channel resistance, we carried out the sensing experiments with 30 cells having various pristine CNN channel resistances as shown in Fig. 3-7. The result clearly shows that the sensitivity is enhanced as the channel resistance increases in the resistance range of 5~30k Ω . Several theoretical and experimental studies have proved that the density of nanotubes in the FET channel plays an important role in transistor performance.^{49,50,51} Our result is consistent with previous works.

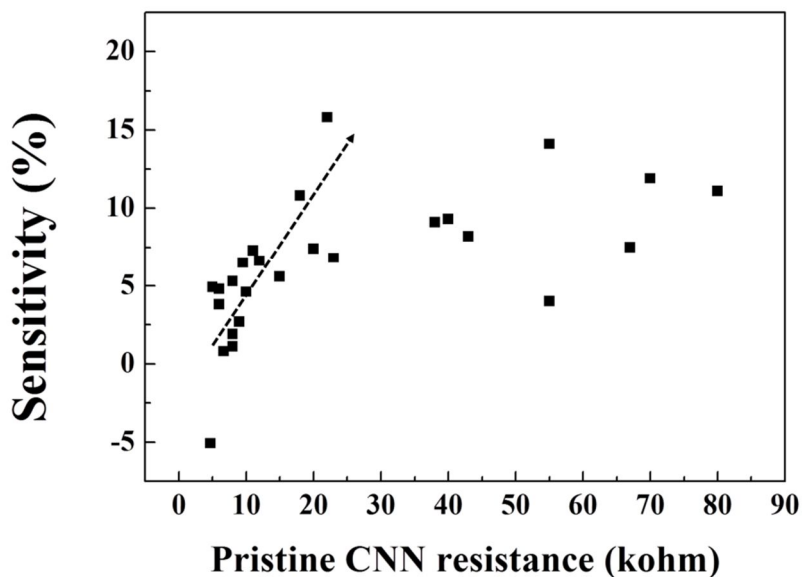


Fig. 3-7. Plots of the sensitivity for each CNN devices with different channel resistance. The sensitivity depends on the channel resistance of CNN-based sensor

For devices with a channel resistance of more than 30k Ω , the sensitivity does not increase anymore contrary to the previous result. We attributed this discrepancy to the reduction of the binding sites (defects) on the CNT surface. Since the number of COOH groups is determined by the number of tubes deposited on the channel region, it is likely that the number of binding sites for antibodies also depends on CNN density. In addition, the number of COOH groups is an uncontrollable parameter in

the fabrication process. The reduction of binding site results in the sensitivity reduction. Therefore, even though the increase of the channel resistance makes the conductance of CNN more semiconductor-like, the sensitivity becomes saturated because the binding sites decrease.

3.4 Conclusion

In summary, the correlation between sensitivity and a channel resistance strongly suggests that the channel resistance will affect the performance of FET device. Thus, we would like to emphasize that the sensitivity to semiconducting property of CNN channel reflects the sensitivity to gating effect by target molecule charge. In addition, the electrostatic gating effect due to the charge of target molecule is the most dominant sensing mechanism in our protein sensor system.

Chapter 4

Carbon nanotube gold island chip: CGI chip

4.1 Introduction

At low nanotube density ($\sim 1 \text{ } \mu\text{m}^{-2}$) the networks are electrically continuous and behave like a p-type semiconductor. At higher densities ($\sim 1 \text{ } \mu\text{m}^{-2}$) the network behaves like a narrow band gap semiconductor with a high off-state current.⁷ In our sensor platform, the sensitivity is enhanced as the channel resistance increases in the resistance range of 5~30k Ω . However, in the high channel resistance regime, we found that the nanotube density does not affect the sensitivity enhancement in

contrary to the previous results. We speculate that a fluctuation of sensitivity is due to the uncertainty on a number of defects at the CNN surfaces.

To improve this issue, we introduced an Au nano-particles (AuNPs) as binding site on CNN-based FET and then compared the device performance with the CNN only devices. We found that AuNPs-CNNFET (CGI chip) shows the good correlation between sensitivity and a channel resistance even though the devices has more than 30k Ω channel resistance. From this work, we propose that AuNPs as binding site is also a critical parameter in achieving high performance of CNT-FET in the high channel resistance regime.

4.2 Effect of AuNPs deposition on the CNN

In order to verify the binding site issue, we introduced Gold Nanoparticles (AuNPs) on the CNNFET by using a thermal evaporation process. The number of COOH groups is significantly dependent on the CNN density, while the number of AuNPs is considerably independent of the CNN density and precisely controllable by the fabrication process. Antibodies are immobilized on the AuNPs by using the thiol-terminated molecule (DTSP) as a linker. The AuNPs-device was incubated with DTSP solution (4 mg/ml^{-1} in dimethyl sulfoxide) during 30min.²⁵ DTSP contains a thiol group which forms the stable S-Au and a highly reactive succinimide ester. An amine group of Antibodies can be covalently bound to NHS ester (DTSP) as shown in Fig. 4-1.

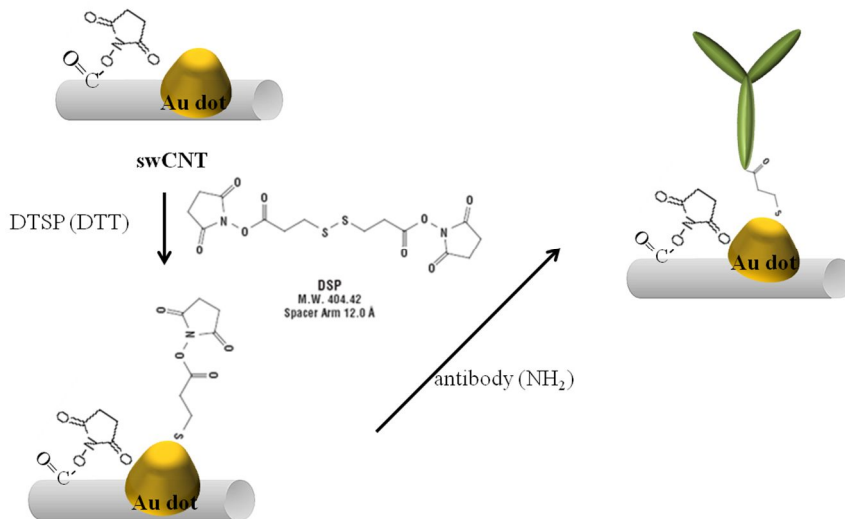


Fig. 4-1. Schematic of an immobilization of antibody on AuNPs-CNN channel

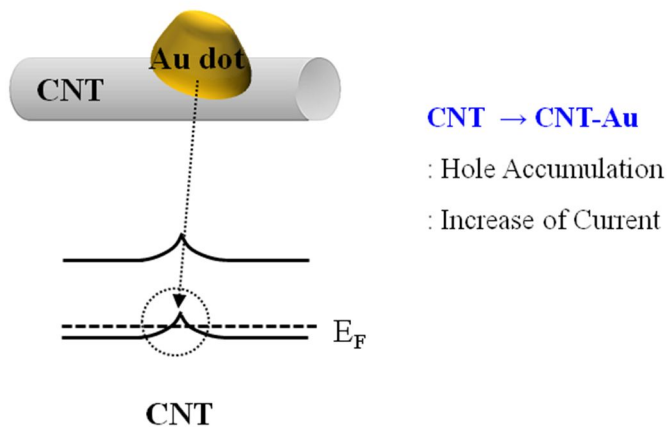


Fig. 4-2. Conceptual scheme illustration of band diagram for the AuNPs deposition on CNN channel

The work function of CNT is 4.8eV which is smaller than that of Au (5.2eV), so hole injection occurs at the Au-CNT contact as shown in Fig. 4-2. Thus, the deposition of AuNPs on the CNN channel can make local accumulation of carriers on the CNN channel and the conductance of CNN channel increases.

4.3 Sensing of microcystin-LR with AuNPs-CNN

4.3.1 I-V characteristics of AuNPs-CNNFET

The change in device current during the surface modification of the AuNPs-CNN device is shown in Fig. 4-3 (a), (b). The measurement result after evaporation of AuNPs shows a significant current increase (about 300%). As shown in Fig. 4-3(c) and (d), the work function of CNT is 4.8eV which is smaller than that of Au (5.1eV), so hole injection occurs at the Au-CNT contact. The deposition of AuNPs on the CNN can make local accumulation of carriers on the CNN channel. After the DTSP treatment, the current decreases about 60% in contrast to the AuNPs-CNN step. This current decrease can be explained by the reduction of the Au work function after binding with the thiol molecules. As shown in Fig. 4-3(e), the schottky barrier on the contact region and the hole depletion in the channel contribute to the current decrease. After antibody immobilization, the current decreases about 15%, which can be explained by decrease in the capacitance between the channel and electrolyte. It is consistent to the case of the CNN device. After antigen-antibody reaction, the enhanced channel current was obtained about 9% with 15k Ω of device as shown in Fig. 4-3 (b). This current increase is also explained by the field effect due to the negative charge of the target molecule.

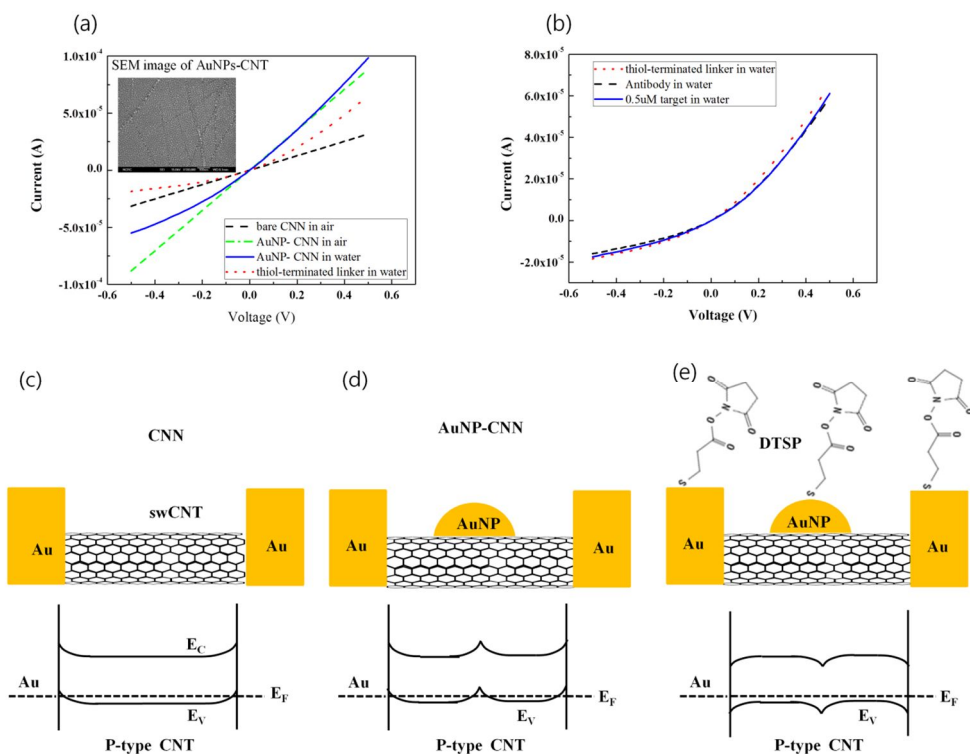


Fig. 4-3. Change in device characteristic $I_{DS}(V_D)$ on modification of the AuNPs-CNN surface. (a) I-V curves of the AuNPs-CNN device for different steps; bare CNN (dash line, black), AuNPs-CNN in air (dash dot line, green), AuNPs-CNN in water (solid line, blue), and thiol-terminated linker (dot line, red). (b) I-V curves of the AuNPs-CNN device for different steps; thiol-terminated linker (dot line, red), after antibody immobilization (dash line, black), and after antigen-antibody reaction (solid line, blue). (c) ~ (e) Schematics and corresponding energy band diagrams of the device (c) CNN device: hole carriers are accumulated by the Au electrode (The work function of Au = 5.1eV, work function of swCNT = ~4.8eV) (d) AuNP-CNN device: hole carriers are accumulated in the vicinity of AuNP on the CNN (e) After

immobilization of DSP (thiol-terminated molecule), the work function of Au is decreased by DTSP. The schottky barrier increased and the hole carriers are depleted.

4.3.2 Effect of thiol-terminated linker (DTSP)

As the thiol-terminated-linker (DTSP) immobilized on the AuNPs, we monitored a decrease in current of CNN channel. The change in current of the CNT-Au system after the binding of thiol molecule can be explained by the work function change of the AuNPs thereby modulating the CNN conductance.^{52,53}

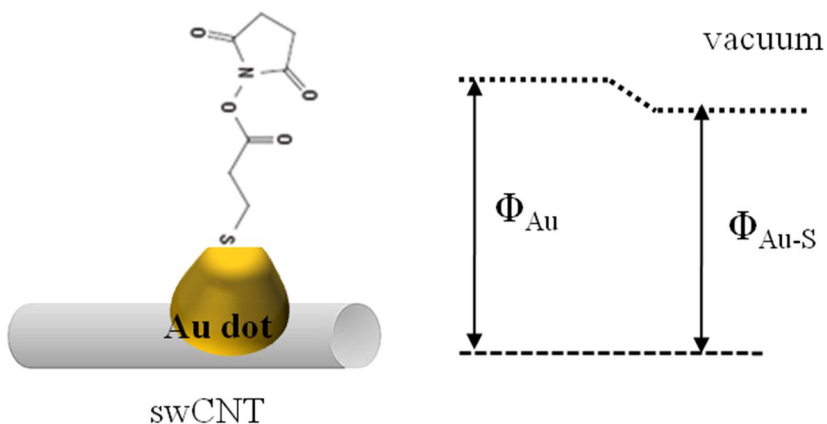


Fig. 4-4. The energy-level alignment at Au-S

4.4 Relationship between the resistance and the sensitivity

The plots of the sensitivity enhancement for several AuNPs decorated devices with various pristine CNN channel resistances. The AuNPs-CNNFETs clearly offer high sensitivity even for a pristine CNN resistance higher than 30k Ω as shown in Fig. 4-5. This is in sharp contrast to the observations in the only CNNFETs.

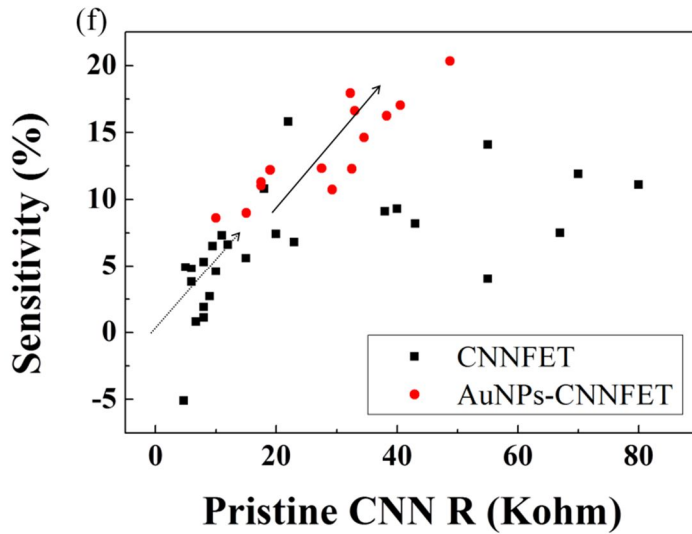


Fig. 4-5. Plots of the sensitivity for two types of devices with different channel resistance. Black are for CNN devices and red are for AuNP-devices.

The density of Au nano-particles in the inset of Fig. 4-3 (a) is about 7.0×10^{11} ea/cm² with the size of 5~7nm. As the size of the antibody is 12nm, only one antibody can be immobilized on one Au nano-particle, in which we can precisely control the number of antibodies on the channel region.

4.5 Conclusion

In this study, we report the importance of the control of the channel resistance of the CNNFET biosensor in the sensitivity. It has been shown that the characteristics of the channel can be modulated efficiently by optimizing the channel resistance. Also, the repeatability is limited by number of the defect sites in the CNN, which may not be easy to control.

However, we have shown that the AuNPs-CNNFET shows reproducible and consistently enhanced sensitivity compared to the CNNFET. Thus it may be concluded that it is critical to carefully tune both CNT channel more semiconducting and the number of binding sites in order to achieve a reliable CNT-FET biosensor.

Chapter 5

MCH passivation of CGI chip: MCH-CGI chip

5.1 Introduction

The significant conductance change of single-walled carbon nanotubes (SWNTs) in response to the physisorption of ammonia and nitrogen dioxide demonstrates their ability to act as sensitive gas sensors.^{54,55,9} This property has been recently demonstrated to be useful to the aqueous solution for bio-molecule detection. Non-specific binding (NSB) on CNT-based biosensor is found to be a general phenomenon. This spontaneous adsorption on CNT surface is attributed to hydrophobic and irreversible interactions in spite of buffer rinsing. However, the

mechanism of how electrical conductance is affected by protein adsorption is currently under debating but necessary to continue efforts to verify it. One proposal for the mechanism is charge donation to nanotubes and the other is schottky barrier modulation at the metal-CNT contact region. Previous studies on protein adsorption have shown that non-specific binding (NSB) results in a decrease in the electrical conductance of the nanotubes. But, the device which the metal-tube contact region are protected from NSB behave significantly differently.¹ Also, in previous reports it has been proposed that the schottky barrier modulation at the contacts is the dominant mechanism from room temperature to 150°C. At higher temperatures, the charge donation process contributes to the response signals.⁵⁵ Various types of chemical materials have been suggested and explored for the blocking layer that can be used in CNT-based biological sensor applications. Using a channel device with passivated CNT/metal contacts by thermally evaporated SiO₂ was suggested for the sensing for NH₃.¹⁹ Poly (methyl methacrylate) (PMMA) was applied to protect for both the metal-CNT contacts and CNT channel.⁵⁶ A selective Si₃N₄ passivation technique was also suggested to protect for both the metal-CNT contacts and CNT channel.⁵⁵ Forming a dense mercapto-hexanol (MCH) layer was introduced onto DNA-modified gold substrates.⁵⁷ As an AuNPs-CCCFET was introduced in previous section, it is necessary to introduce thiol-terminated blocking layer that can serve as a specific anchor to covalently tether on Au electrode surface by self-assembly from solution. Therefore, we introduce 6-mercapto-hexanol (MCH) on the CGI chip to passivate the Au electrode surface.

5.2 The formation of MCH SAM on Au-nanotube contact region

The blocking layer structure should be modified a thiol linker, which can support a covalent bond with Au electrode. A conceptual scheme of a MCH treated AuNPs CNNFET, as shown in Fig. 5-1. A MCH treatment is composed of three different surface modification process. The substrates are cleaned by O₂ plasma process and 15min of sonication process and, prior to CNT coating, follow by a final rinse with distilled water. A CNN channel formation is accomplished by dip coating process. Followig CNT coating process, the CNNFET is subjected to a second adsorption step by exposing it to MCH ([MCH] = 0.5mM, 12h exposure time), which leads to the formation of a MCH monolayer.⁵⁸ After then, AuNPS are deposited on CNN channel by thermal evaporation, as shown in Fig. 5-2.

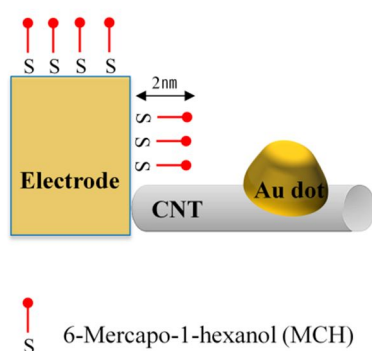


Fig. 5-1. Conceptual scheme of a MCH treated AuNPs CNNFET

■ Device Fabrication

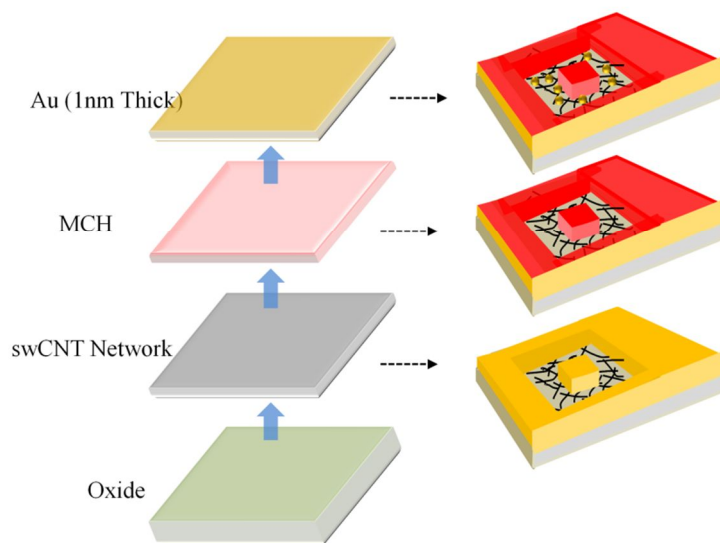
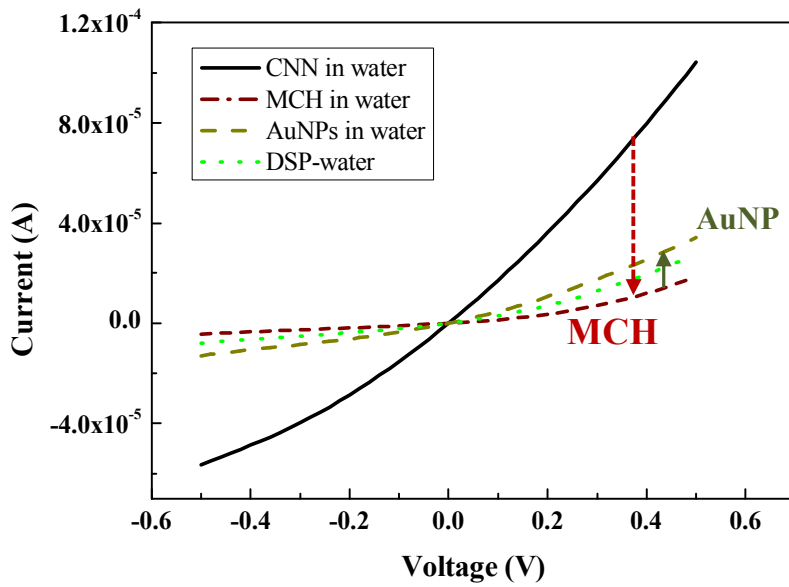


Fig. 5-2. Conceptual scheme of fabrication flow of three different surface modifications

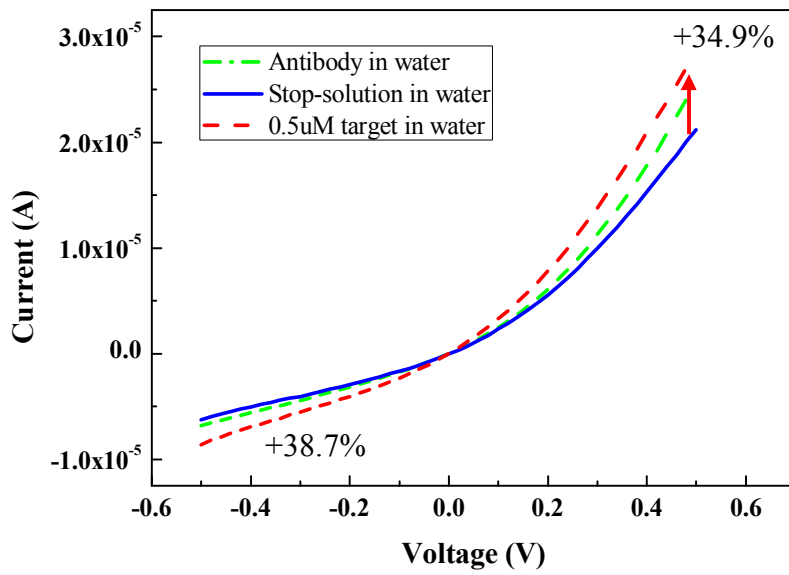
5.3 Sensing of microcystin-LR with MCH treated AuNPs-CNNFET

In order to investigate the effect of blocking for NSB of MCH monolayer on the Au-nanotube contact region, a microcystin-LR sensing was carried out with MCH treated AuNPs-CNNFET (MCH-CGI chip) in distilled water. We measured the current change of the MCH-CGI chip for each step during surface modifications; pristine CNN, MCH treatment, AuNPs deposition, stop-solution, immobilization of antibody, and after antigen-antibody reaction as shown in Fig. 5-3 (a) and (b). Before the measurement of each step, the device was rinsed and incubated with distilled water.

After MCH treatment, a significant current decrease was observed, which can be explained by the reduction of the Au work function after binding with the thiol molecules. The deposition of AuNPs on the MCH treated CNN can make local accumulation of carriers on the CNN channel. After the DTSP treatment, the current also decreases due to the reduction of the Au work function. After antigen-antibody reaction, the channel current sharply increased about 39% with 10k Ω of device as shown in fig. 5-3 (b). We would like to emphasize that this outstanding enhanced sensitivity to the introduction of MCH monolayer as a blocking layer. NSB on the Au-nanotube contact region is the key to conductance modulation and electrical sensing. Schottky barrier of Au-nanotube contact leads to a significant decrease in conductance and a suppressed sensitivity.



(a)



(b)

Fig. 5-3. (a) Change in device characteristic I_{DS} (V_D) on pre-treatment of the MCH-AuNPs-CNN; pristine CNN (solid line, black), MCH-CNN (dash dot line, brown), MCH-AuNPs-CNN (dash line, yellow green), and thiol-terminated liner (dot line, green). (b) I-V curves on sensing measurement of the MCH-AuNPs-CNN device; after antibody immobilization (dash dot line, green), after stop solution (solid line, blue), and after antigen-antibody reaction (dash line, red).

The work function of CNT is 4.8eV which is smaller than that of Au (5.1eV), so hole injection occurs at the Au-CNT contact in CNNFET, as shown in fig. 5-4 (a).

After the MCH treatment, the current decreases and this current decrease can be explained by the reduction of the Au work function after binding with the thiol molecules. The work function of Au becomes smaller than that of CNT, so schottky barrier increases at the Au-CNT contact in CNNFET as shown in fig. 5-4 (b). However, the deposition of AuNPs on the MCH-CNNFET can induce a local accumulation of carriers on the CNN channel, as shown in fig. 5-4 (c). The conductance of CNN increases. After the DTSP treatment, the conductance decreases about 60% in contrast to the AuNPs-CNN step. The holes are depleted in the channel and the conductance of channel decreases, as shown in fig. 5-4 (d).

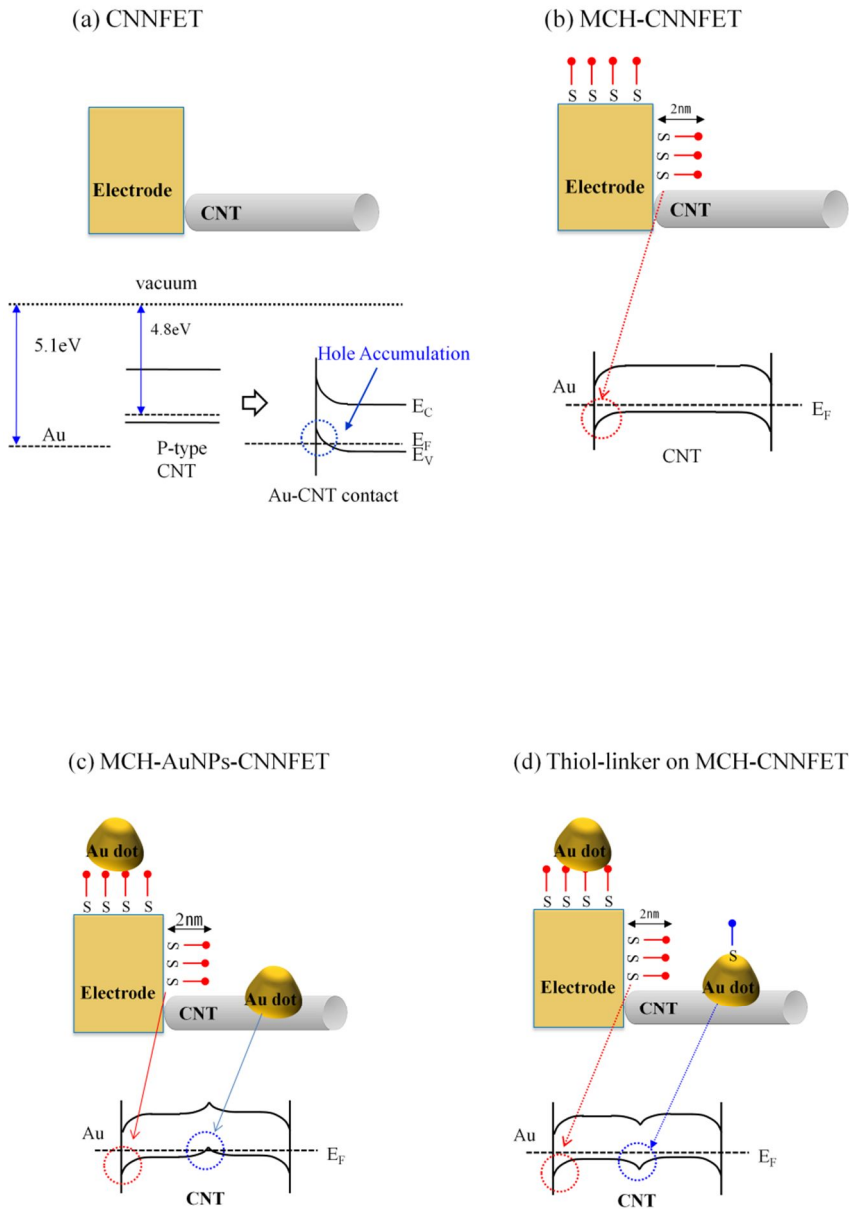


Fig. 5-4. Energy-level alignments during the surface modifications

5.4 Conclusion

To verify the MCH monolayer to prevent a non-specific binding, sensing experiments were performed with Au electrode-passivated devices. Even though MCH treatment, non-specific binding occurred significantly on the bare CNT surfaces. However, the MCH treated AuNPs-CNNFET exhibited an outstanding enhanced sensitivity. We attribute this sensitivity enhancement to the elimination of NSB on Au electrode-CNT contact. These experiments clearly demonstrated the importance of passivation on Au electrode-CNT contact region. Contact region is highly susceptible to Schottky barrier modulation by protein adsorptions.

Based on these results, we propose that the electrical property of the Au electrode-nanotube contact may be modulated by protein adsorption and this change reflects a reduction of the Au work function. Therefore, p-type CNNFET should exhibit a conductance decrease due to protein NSB on Au-CNT contact.

Chapter 6

Conclusion

6.1 Summary

In the study, the sensitivity enhancement method adopting CNN based sensor platform has been introduced and experimentally verified. For the electrical detection of microcystin-LR, the sensor platform was developed by the capping of the defects on the CNN channel, the deposition of AuNPs as binding sites, and the passivation of a metal-nanotube contact.

The carboxylated CNN channel was modulated depending on pH condition in an aqueous solution. We blocked the CNT defects to make the CNT device insensitive to the pH condition. As the unwanted side reactions were reduced by the surface treatments of the oxide and CNTs, reliable operation and sensitivity of the sensor could be guaranteed.

To detect microcystin-LR with a CNNFET, we show the importance for the semiconducting property of CNN channel in sensitivity. In addition, we introduced AuNPs on a CNN channel (CGI chip) as binding sites. Compared with a CNNFET, a consistently enhanced sensitivity and repeatability were obtained with an AuNPs-

CNNFET.

To eliminate the protein adsorptions on Au-nanotube contact regions and source drain electrodes, the MCH layer was introduced as blocking layer. The decrease in conductance due to schottky barrier modulation was suppressed by MCH passivations and, thus the enhanced sensitivity was achieved.

By combining the AuNPs and MCH SAM, we successfully developed a protein sensor platform and clearly enhanced the sensitivity of microcystin-LR.

6.2 Pulsed measurement of the transient state

A FET device basically is a surface-charge measuring device, and immuno-FET should detect electrically charged molecules. the antibody-antigen reaction induce the modulation of the carrier density and the conductivity in the semiconductor channel. Under ideal conditions, the immunoFET detects a highly charged antigens with the very low ionic strength, as shown in Fig. 6-1(a). However, the principle practical problem is to detect a low charged antigens in high ionic strength solutions, as shown in Fig. 6-1(b). It is obvious that the potential (charge) is fundamentally impeded by the ionic screening.^{59,60,12,61} An antibody normally is much longer than electric double layer (EDL) and the protein charge is shielded by counter ions in ionic solution. In this study, we propose a new sensing method based on ‘the transient state’ measurement. A concept of transient state measurement was introduced in Jun-

Myung Woo's PhD dissertation. The electrical current is measured after the step voltage is applied between the channel and the electrolyte solution. In initial steady state, both the CNN channel surface and the charged target molecule are screened by the counter-ions. The counter-ions (H^+) are swept away by high external electric field and the charged molecules efficiently affect on the semiconductor surface until the screening ions are redistributed.

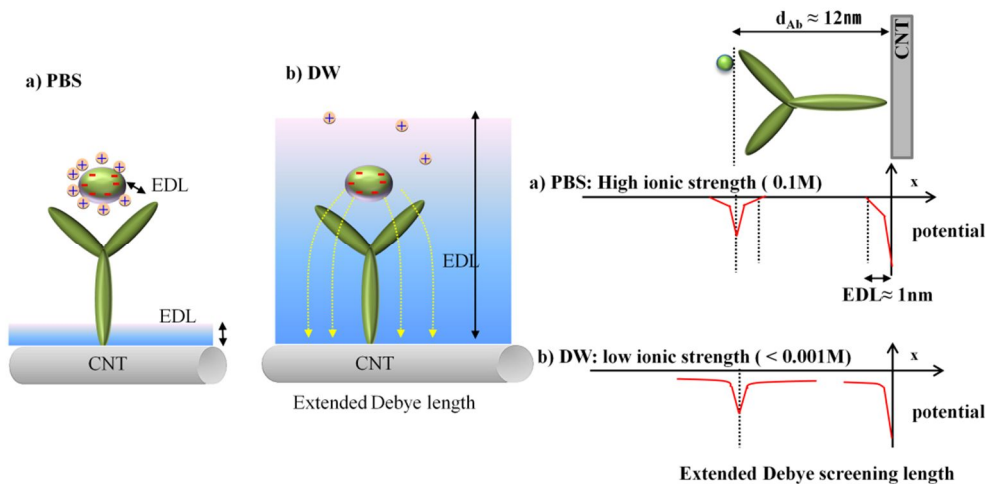


Fig. 6-1. Schematics of the potential distribution in an electrolyte (a) low ionic strength (b) high ionic strength

We investigated the sensing performance to detect a microcystin-LR in PBS by the transient measurement. After the charging current is subtracted in the output of the operational amplifier, we obtain the transient response of channel conductance after application of 0.5 V unit voltage. Fig. 6-2 shows the transient response of the MCH treated AuNPs-CNNFET before (antibody) and after (microcystin) reaction. Antibody-antigen immuno-reaction is performed in with 0.5 μM target concentration during 15 min.

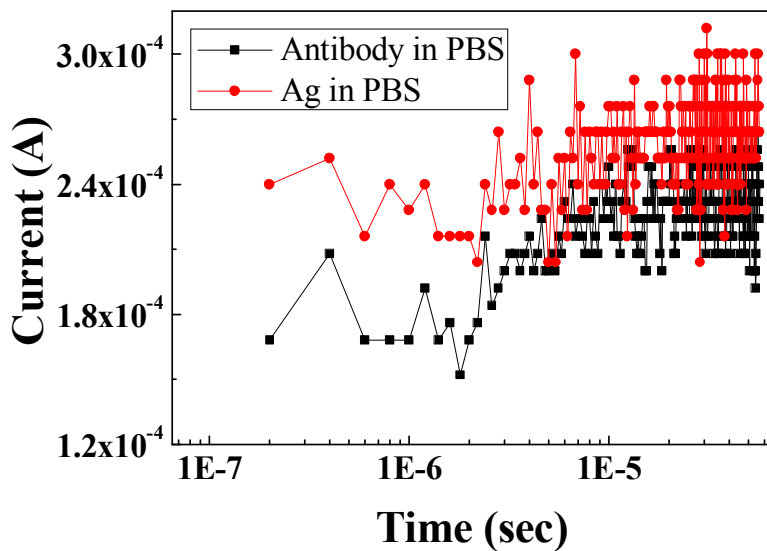


Fig. 6-2. Comparison of transient response between antibody and antigen after the unit voltage applied.

As a control experiment , the current change was measured after washing with PBS by transient measurements before and after antibody-antigen reaction. Comparing the transient responses of the channel current, the sensitivity in the transient states can be plotted as shown in Fig. 6-3. The sensitivity becomes maximum between 100 ns and 1 μ s after application of the unit pulse.

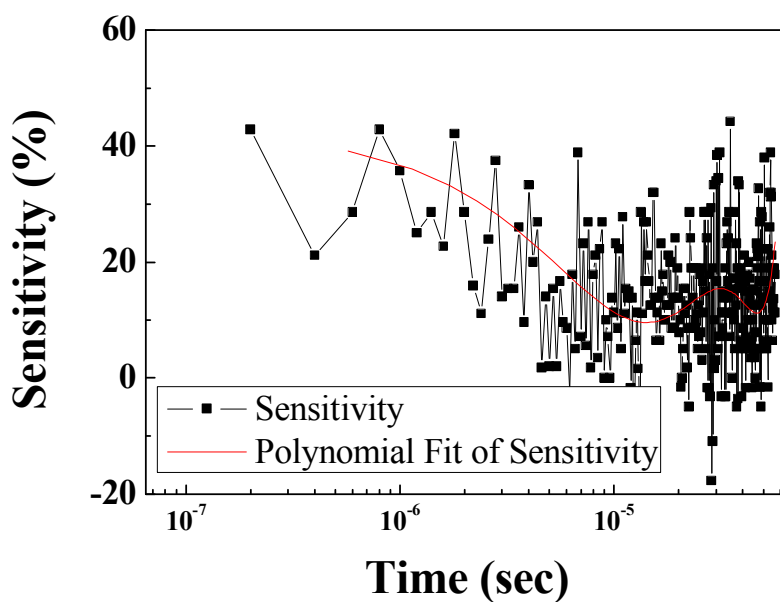


Fig. 6-3 Sensitivity enhancement by transient measurement after 0.5V unit voltage applied.

The use of PBS (high ionic strength) severely restricts the charge of target molecule to reach the CNN channel surface because protein charge is shielded by counter ions in PBS. However, we are able to achieve an enhanced sensitivity even compared with a sensitivity in distilled water by applying the transient electrical measurement. This experiment demonstrates that the transient measurement can mitigate the charge screening effect in the electrical biosensor.

6.3 Future Works

In the dissertation, we show a new sensor platform to overcome the limitation of electrical biosensor. For the future study of the present work, we may extend the present work to several valuable applications. First, it should be necessary to verify an accurate sensing mechanism about the electrical physics between antibody-antigen reaction and CNN channel. Second, the sensing measurement may be extended to sensing event under human serum instead of distilled water or PBS. Finally, more fundamental studies should be performed in terms of the relationship between the mechanical motion of the biomolecules and frequency of the pulse trains.

References

- ¹ Robert J. Chen, Hee Cheul Choi, Sarunya Bangsaruntip, Erhan Yenilmez, Xiaowu Tang, Qian Wang, Ying-Lan Chang, and Hongjie Dai, *Journal of the American Chemical Society* **126** (5), 1563 (2004).
- ² Iddo Heller, Sohail Chatoor, Jaan Männik, Marcel A. G. Zevenbergen, Cees Dekker, and Serge G. Lemay, *Journal of the American Chemical Society* **132** (48), 17149 (2010).
- ³ M. S. Dresselhaus, G. Dresselhaus, R. Saito, and A. Jorio, *Physics Reports* **409** (2), 47 (2005).
- ⁴ Kannan Balasubramanian and Marko Burghard, *Small* **1** (2), 180 (2005).
- ⁵ F.N. Ishikawa, M. Curreli, C.A. Olson, H.I. Liao, R. Sun, R.W. Roberts, R.J. Cote, M.E. Thompson, and C. Zhou, *ACS nano* (2010).
- ⁶ S. Kumar, N. Pimparkar, JY Murthy, and MA Alam, *Applied physics letters* **88**, 123505 (2006).
- ⁷ ES Snow, JP Novak, PM Campbell, and D. Park, *Applied Physics Letters* **82**, 2145 (2003).
- ⁸ M.A. Topinka, M.W. Rowell, D. Goldhaber-Gordon, M.D. McGehee, D.S. Hecht, and G. Gruner, *Nano letters* **9** (5), 1866 (2009).
- ⁹ G. Gruner, *Anal Bioanal Chem* **384** (2), 322 (2006).
- ¹⁰ K. Maehashi and K. Matsumoto, *Sensors* **9** (7), 5368 (2009).
- ¹¹ M. Lee, J. Im, BY Lee, S. Myung, J. Kang, L. Huang, Y.K. Kwon, and S. Hong, *Nature nanotechnology* **1** (1), 66 (2006).
- ¹² E. Stern, R. Wagner, F.J. Sigworth, R. Breaker, T.M. Fahmy, and M.A. Reed, *Nano letters* **7** (11), 3405 (2007).
- ¹³ M. Lee, K.Y. Baik, M. Noah, Y.K. Kwon, J.O. Lee, and S. Hong, *Lab Chip* **9** (16), 2267 (2009).
- ¹⁴ Yiping Chen, He ling Ren, Nan Liu, Na Sai, Xiaoyu Liu, Zhen Liu, Zhixian Gao, and Bao an Ning, *Journal of Agricultural and Food Chemistry* **58** (16), 8895 (2010).
- ¹⁵ Jun Pyo Kim, Byung Yang Lee, Seunghun Hong, and Sang Jun Sim, *Analytical Biochemistry* **381** (2), 193 (2008).
- ¹⁶ Fang Yu, Björn Persson, Stefan Löfås, and Wolfgang Knoll, *Analytical Chemistry* **76** (22), 6765 (2004).

- 17 X. Yu, B. Munge, V. Patel, G. Jensen, A. Bhirde, J.D. Gong, S.N. Kim, J.
Gillespie, J.S. Gutkind, and F. Papadimitrakopoulos, *Journal of the
American Chemical Society* **128** (34), 11199 (2006).
- 18 Yongki Choi, Issa S. Moody, Patrick C. Sims, Steven R. Hunt, Brad L.
Corso, Israel Perez, Gregory A. Weiss, and Philip G. Collins, *Science* **335**
(6066), 319 (2012).
- 19 Keith Bradley, Jean-Christophe P. Gabriel, Mikhail Briman, Alexander Star,
and George Grüner, *Physical Review Letters* **91** (21), 218301 (2003).
- 20 K. Bradley, M. Briman, A. Star, and G. Grüner, *Nano Letters* **4** (2), 253
(2004).
- 21 Chao Gao, Zheng Guo, Jin-Huai Liu, and Xing-Jiu Huang, *Nanoscale* **4**
(6), 1948 (2012).
- 22 Minh-Phuong Ngoc Bui, Xuan-Hung Pham, Kwi Nam Han, Cheng Ai Li,
Eun Kyu Lee, Ho Jung Chang, and Gi Hun Seong, *Electrochemistry
Communications* **12** (2), 250 (2010).
- 23 Khaled A. Mahmoud, Sabahudin Hrapovic, and John H. T. Luong, *ACS
Nano* **2** (5), 1051 (2008).
- 24 Xing-Jiu Huang, Cun-Cheng Li, Bonsang Gu, Ju-hyun Kim, Sung-Oh Cho,
and Yang-Kyu Choi, *The Journal of Physical Chemistry C* **112** (10), 3605
(2008).
- 25 Rouslan V. Olkhov, Jeremy D. Fowke, and Andrew M. Shaw, *Analytical
Biochemistry* **385** (2), 234 (2009).
- 26 Christopher B. Jacobs, M. Jennifer Peairs, and B. Jill Venton, *Analytica
Chimica Acta* **662** (2), 105 (2010).
- 27 HYE RYUNG BYON, SUPHIL KIM, and HEE CHEUL CHOI, *Nano* **03**
(06), 415 (2008).
- 28 J.H. Cheon, J. Lim, S.M. Seo, J.M. Woo, S.H. Kim, Y. Kwon, J.W. Ko, T.J.
Kang, Y.H. Kim, and Y.J. Park, *Electron Devices, IEEE Transactions on*
57 (10), 2684 (2010).
- 29 E.Y. Jang, T.J. Kang, H.W. Im, D.W. Kim, and Y.H. Kim, *Small* **4** (12),
2255 (2008).
- 30 Qing Cao and John A. Rogers, *Advanced Materials* **21** (1), 29 (2009).
- 31 P. Bergveld, R. E. G. van Hal, and J. C. T. Eijkel, *Biosensors and
Bioelectronics* **10** (5), 405 (1995).
- 32 R. E. G. van Hal, J. C. T. Eijkel, and P. Bergveld, *Sensors and Actuators B:
Chemical* **24** (1–3), 201 (1995).
- 33 M. Grattarola, G. Massobrio, and S. Martinoia, *Electron Devices, IEEE
Transactions on* **39** (4), 813 (1992).
- 34 P. Bergveld, *Sensors and Actuators B: Chemical* **4** (1–2), 125 (1991).
- 35 P. Bergveld, *Sensors and Actuators B: Chemical* **88** (1), 1 (2003).
- 36 Hung-Kwei Liao, Li-Lun Chi, Jung-Chuan Chou, Wen-Yaw Chung, Tai-
Ping Sun, and Shen-Kan Hsiung, *Materials Chemistry and Physics* **59** (1),
6 (1999).
- 37 P. Bergveld, *Sensors and Actuators A: Physical* **56** (1–2), 65 (1996).

38 A. Simon, T. Cohen-Bouhacina, M. C. Porté, J. P. Aimé, and C. Baquey,
Journal of Colloid and Interface Science **251** (2), 278 (2002).

39 Xiaolin Zhao and Raoul Kopelman, The Journal of Physical Chemistry
100 (26), 11014 (1996).

40 M. Joshi, M. Goyal, R. Pinto, and S. Mukherji, presented at the Computer
Architectures for Machine Perception, 2003 IEEE International Workshop
on, 2004 (unpublished).

41 Qiang Fu, Chenguang Lu, and Jie Liu, Nano Letters **2** (4), 329 (2002).

42 D. Lee and T. H. Cui, J. Vac. Sci. Technol. B **27** (2), 842 (2009).

43 Dongjin Lee and Tianhong Cui, 2009 (unpublished).

44 Dongjin Lee and Tianhong Cui, Biosensors and Bioelectronics **25** (10),
2259 (2010).

45 J.P. Kim, B.Y. Lee, J. Lee, S. Hong, and S.J. Sim, Biosensors and
Bioelectronics **24** (11), 3372 (2009).

46 Dong Wan Kim, Gyu Sik Choe, Sung Min Seo, Jun Ho Cheon, Hansuk Kim,
Jung Woo Ko, In Young Chung, and Young June Park, Applied Physics
Letters **93** (24), 243115 (2008).

47 G.S. Shephard, S. Stockenström, D. de Villiers, W.J. Engelbrecht, and G.F.S.
Wessels, Water Research **36** (1), 140 (2002).

48 Brett R. Goldsmith, John G. Coroneus, Alexander A. Kane, Gregory A.
Weiss, and Philip G. Collins, Nano Letters **8** (1), 189 (2007).

49 N. Pimparkar, Guo Jing, and M. A. Alam, Electron Devices, IEEE
Transactions on **54** (4), 637 (2007).

50 P. R. Nair and M. A. Alam, Applied Physics Letters **88** (23), 233120
(2006).

51 S. Myung, M. Lee, G. T Kim, J. S Ha, and S. Hong, Advanced Materials
17 (19), 2361 (2005).

52 Xiaodong Cui, Marcus Freitag, Richard Martel, Louis Brus, and Phaedon
Avouris, Nano Letters **3** (6), 783 (2003).

53 Jung Woo Ko, Jun-Myung Woo, Ahn Jinhong, Jun Ho Cheon, Jae Heung
Lim, Seok Hyang Kim, Honggu Chun, Eunhye Kim, and Young June Park,
ACS Nano **5** (6), 4365 (2011).

54 Bo Pan and Baoshan Xing, Environmental Science & Technology **42** (24),
9005 (2008).

55 Ning Peng, Qing Zhang, Chee Lap Chow, Ooi Kiang Tan, and Nicola
Marzari, Nano Letters **9** (4), 1626 (2009).

56 Jian Zhang, Anthony Boyd, Alexander Tselev, Makarand Paranjape, and
Paola Barbara, Applied Physics Letters **88** (12), 123112 (2006).

57 K. Arinaga, U. Rant, M. Tornow, S. Fujita, G. Abstreiter, and N. Yokoyama,
Langmuir **22** (13), 5560 (2006).

58 U. Rant, K. Arinaga, S. Fujita, N. Yokoyama, G. Abstreiter, and M. Tornow,
Nano Letters **4** (12), 2441 (2004).

59 Alexander Star, Jean-Christophe P. Gabriel, Keith Bradley, and George
Grüner, Nano Letters **3** (4), 459 (2003).

- ⁶⁰ Sebastian Sorgenfrei, Chien-yang Chiu, Matthew Johnston, Colin Nuckolls, and Kenneth L. Shepard, *Nano Letters* **11** (9), 3739 (2011).
- ⁶¹ Guo-Jun Zhang, Gang Zhang, Jay Huiyi Chua, Ru-Ern Chee, Ee Hua Wong, Ajay Agarwal, Kavitha D. Buddharaju, Navab Singh, Zhiqiang Gao, and N. Balasubramanian, *Nano Letters* **8** (4), 1066 (2008).

초 록

전기적 단백질 센서가 많은 연구에도 불구하고 실용화를 하지 못하고 있는 것은 낮은 감도와 선택 도에 그 원인이 있으며, 그 중 낮은 감도는 비특이 반응과 반대이온의 전하 차단 효과에 의한 전기적 신호의 약화에 기인한다.

본 논문에서는 전기적 단백질 센서의 낮은 감도 현상이 개선된 센서 플랫폼의 개발 방법을 제안한다. 이에 대한 연구 진행을 위하여, 마이크로 시스틴을 타겟 물질로, 마이크로 시스틴 항체를 프로브 물질로 선정하였다. 또한 마이크로 시스틴은 수질 오염 여부를 판단하는 단백질 표지인자이므로, 이에 대한 검출 실험은 증류수에서 진행하였다.

센서 플랫폼을 개발하기 위한 연구는 세가지 방향에서 진행되었다. 가장 먼저 수용액상에서 탄소 나노 튜브 채널의 전기적 안정성을 확보하기 위하여, 센서 표면에 존재하는 실라놀 기능기와 탄소 나노 튜브 표면에 존재하는 카르복실 기능 기에 특성을 연구하였다. 그래서 버퍼 용액이나 증류수 상에서 탄소 나노 튜브 기반의 센서가 전기적으로 안정적인 특성을 보이도록 개선하였다.

두 번째로는, 탄소나노 튜브 채널 저항 조절을 통하여 탄소나노 튜브의 농도를 조절할 수 있었고, 채널 저항 증가와 채널의 반도체 특성과의 관계를 밝힘으로써 탄소 나노 튜브 기반 센서의 민감도를 향상 시킬 수 있었다. 그런데, 탄소 나노 튜브 기반 센서는 높은 채널 저항 영역에서 민감도의 재현성이 감소하는 좋지 않은 특성을 보여 주며, 이에 대한 개선이 필요하였다. 그래서 이러한 단점을 개선하기 위하여 금 나노 입자를 나노 튜브 채널에 도입하여 항체 고정화 사이트로 활용하였고, 이렇게 제조된 나노 스케일의 금 입자가 부착된 탄소 나노 튜브 센서는 민감도와 재현성 두 가지 측면에서의 향상된 특성을 얻을 수 있었다.

마지막으로, 비특이 반응에 의한 민감도 저하 현상은 단백질 센서의 민감도 저하 현상을 유발하므로 이에 대한 연구를 진행하였다. 비특이 반응

에 의한 채널 전류 감소 현상은 특히 금 전극과 나노 튜브 접촉면에서 크게 발생하므로, 이에 대한 개선책으로 6-mercapto-hxanol (MCH)를 blocking layer 로 센서에 적용하였다. MCH 로 전극/ 나노 튜브 접촉영역에서의 비특이 반응을 방지함으로써 schottky barrier 에 의한 채널 전류 감소 현상을 제거할 수 있었고, 이것은 바로 민감도의 향상으로 연결되어 MCH 처리된 탄소 나노 튜브 센서에서 현격한 민감도 향상을 얻을 수 있었다.

본 연구를 통하여 우리는 카본 나노 튜브를 기반으로 한 단백질 센서 플랫폼을 개발하였고, 이를 이용하여 다양한 단백질 물질들에 대해 충분한 감도와 신뢰성을 갖는 실시간 전기적 검출을 진행하는데 기여할 수 있을 것으로 기대한다.

주요어: 단백질 센서, 카본 나노 튜브 채널, 금 나노 입자, MCH, 민감도.

학번: 2008-30209